3rd Trilateral International Workshop on Energetic Particle Physics

Overview of KSTAR experiments on EP and diagnostics status

7th Nov 2022, Zoom Online organized by ENEA, Italy

J. Kim[1], J. Kang[1], T. Rhee[1], K. Kim[1], J. Jo[1], K. Ogawa[2], M. Isobe[2], M. Podesta[3], M.W. Lee[4], and collaborators

[1]KFE, [2]NIFS, [3]PPPL, [4]KAIST

Contents

- Experimental study of EP physics in KSTAR plasmas
- Status of diagnostic set-up to support the EP experiments

1. Experimental topics of KSTAR EP research

- Research topic selection is based on the ITPA EP joint experiments list.
- Fast-ion loss w/ RMP (EP6)
- Alfvén eigenmode control (EP10, EP12)
- Triton burnup

KFE
한국핵융합에너지연구원
KOREA INSTITUTE OF FUSION ENERGY

Fast-ion loss under the 3-D field applications

associated with RMP-ELM control experiments

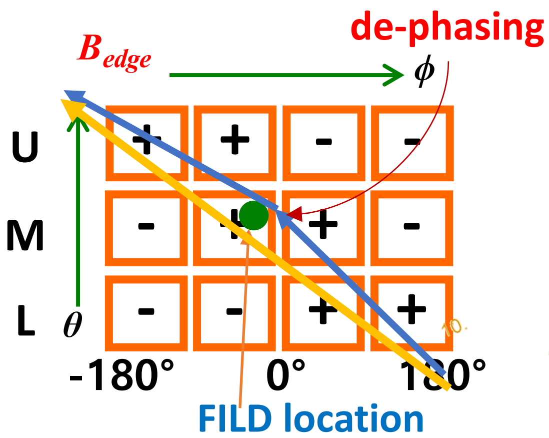

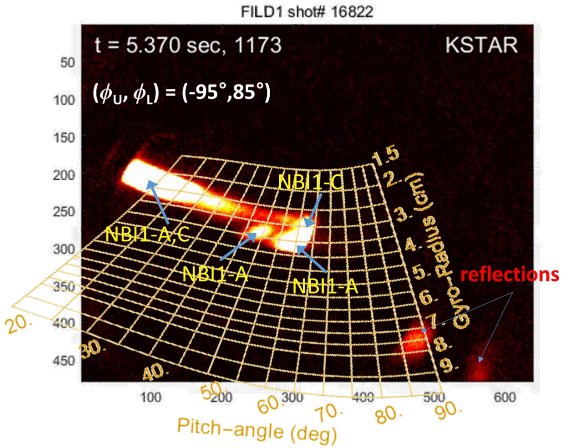

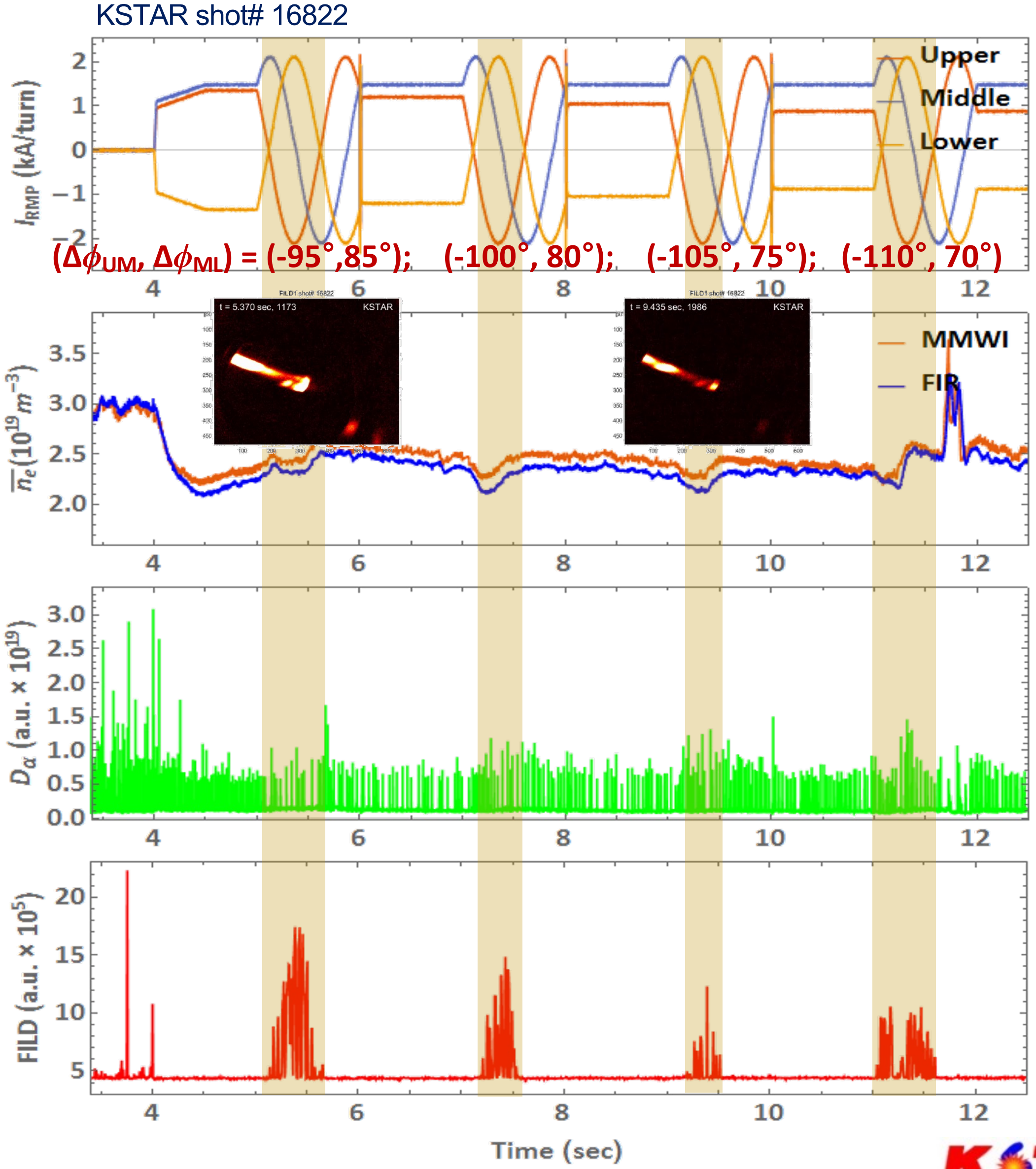

- Poloidal spectrum of *n=1* 3-D field is applied. (intentionally misaligned configuration: **Non-equal phasing ($\varphi_{UM} \neq \varphi_{ML}$) 3-D configurations that require the presence of the 3rd row. → in support of ITER**)
- Dephasing is useful to control the fast-ion losses while the ELM is controlled. (J. Kim *et al.*, 15th IAEA TM on EP (2017))
- ***Reduction of localized fast-ion loss (change in P_φ) by dephasing***

Fast-ion loss under the 3-D field applications

associated with RMP-ELM control experiments

- **" Intentionally misaligned" (dephasing) RMP** (*n*=1, +90° base) applications using all three rows (Top-Middle-Bottom): have shown the **reduction of the localized fast-ion losses**, **depending on the phasing angle**.

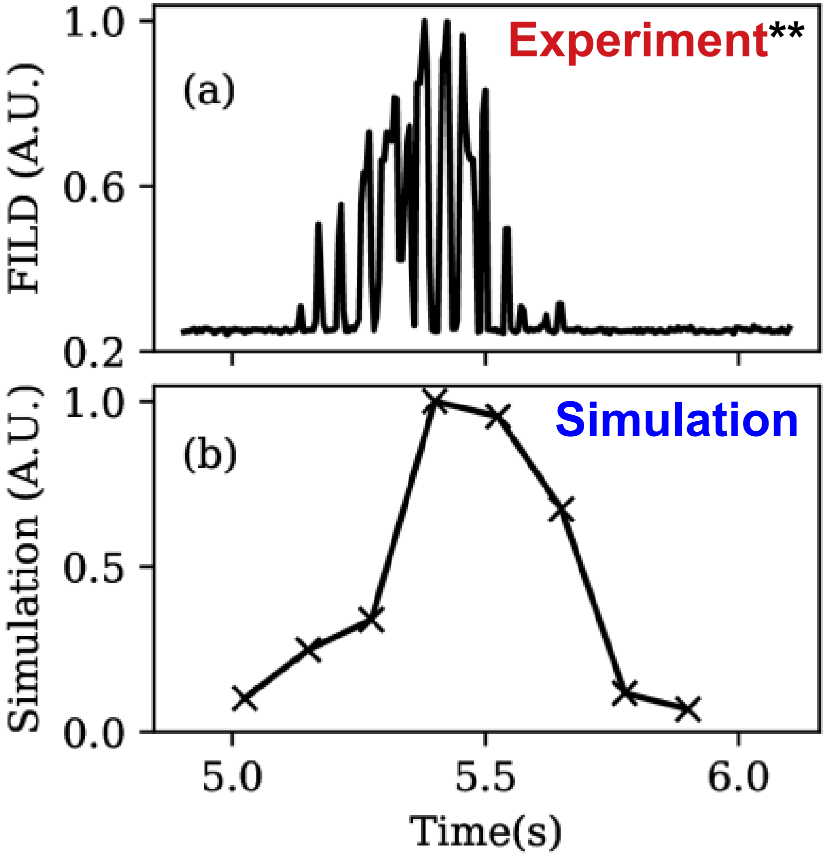

See the details. (**T. Rhee** et al., at this conference)

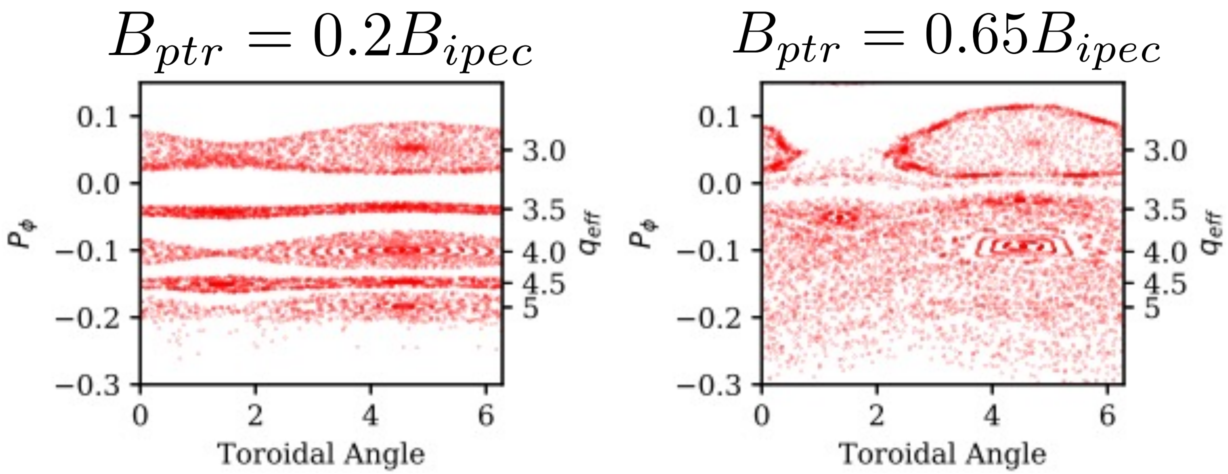

- Orbit simulations (NuBDeC*) reveal that the **resonant orbit-stochastization at the edge by the external 3D field** makes the shortcut to the wall.
- Fast-ion loss intensity depends on perturbation amplitude and toroidal location.**

*T. Rhee *et al.*, PoP **26** 112504 (2019)
T. Rhee *et al.*, NF **62 066028 (2022)

Fast-ion loss under the 3-D field applications

associated with RMP-ELM control experiments

(using the **3-row coils**, reverse dephasing, <u>n=1, +90° phasing</u>)

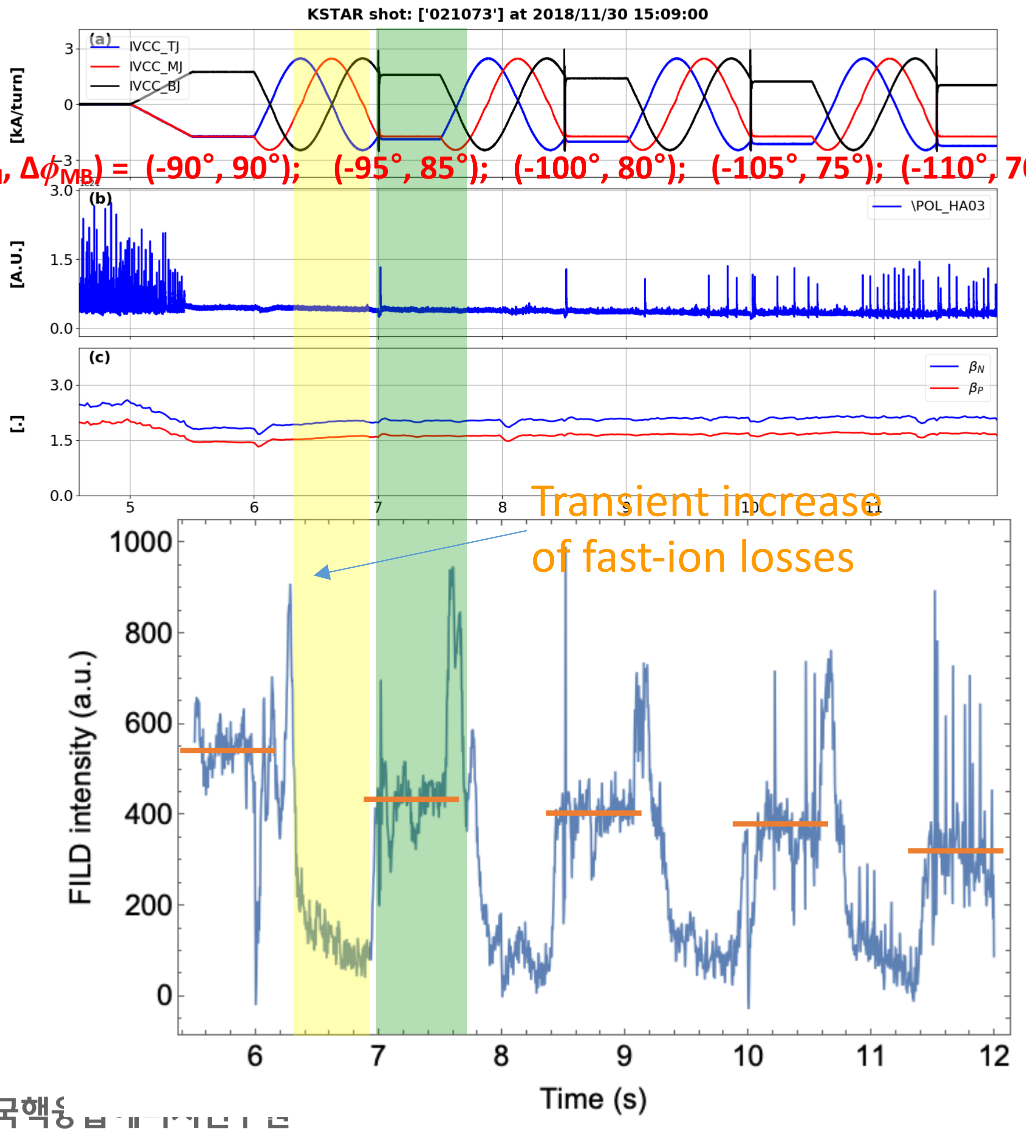

(using the **2-row coils (T-M, M-B)**, <u>n=1, +90° phasing</u>)

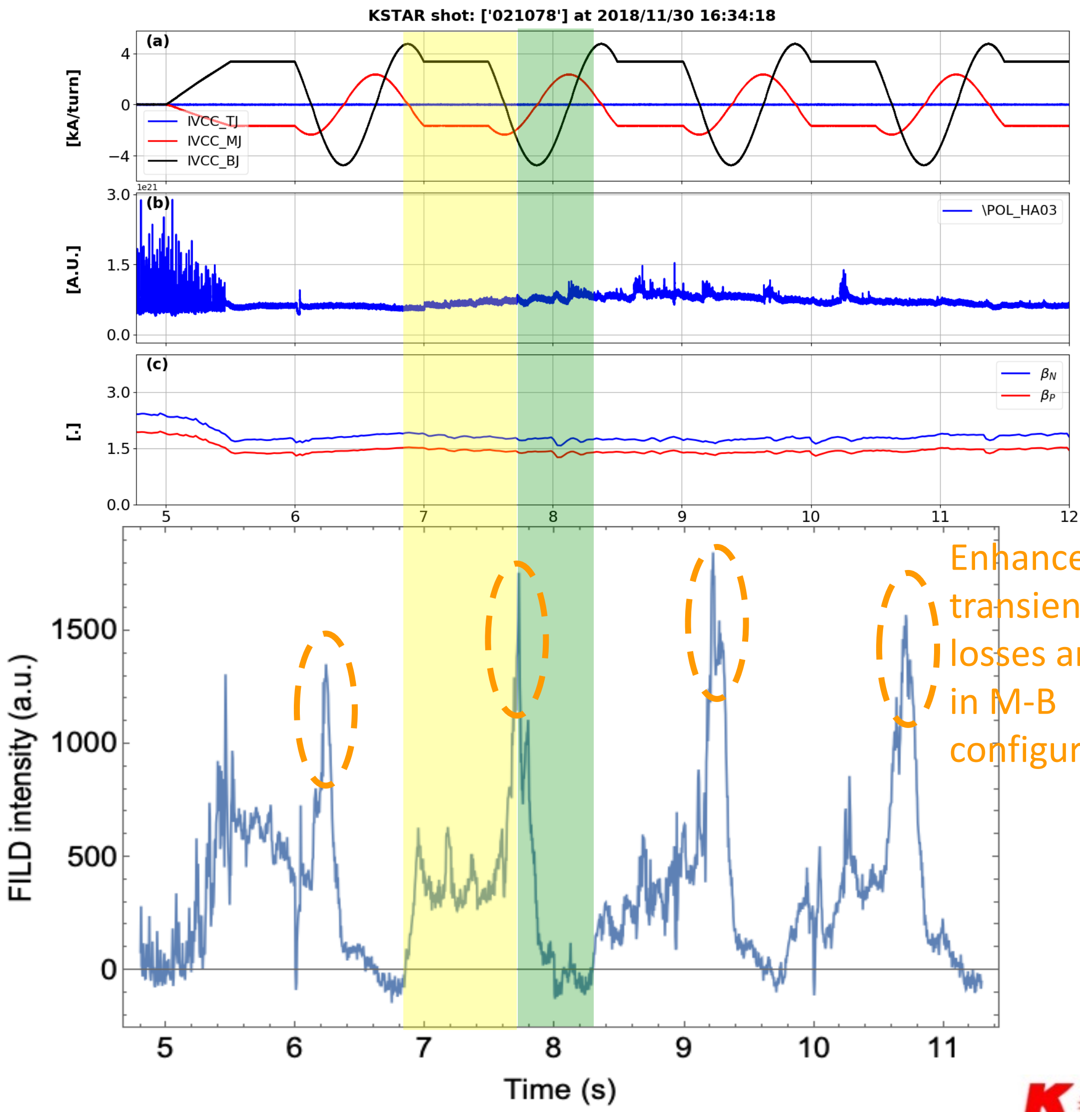

Enhanced transient fast-ion losses are found in M-B configuration.

Fast-ion loss under the 3-D field applications

associated with RMP-ELM control experiments

- **”Intentionally misaligned” (dephasing) RMP** (n=1, +90° base) applications using all three rows (Top-Middle-Bottom): have shown the **reduction of the localized fast-ion losses, depending on the phasing angle**.
- **Extended experiments (three-rows RMP) have shown that dephasing of RMP is also applicable to the ELM-suppression conditions.**
- **Transient increase in fast-ion loss in the narrow poloidal spectrum window needs to be avoided even in slowly-rotating RMP configurations.**
- ***Plasma response modelling is being done to characterize and quantify the optimal RMP poloidal spectrum.***
- ***Orbit-following modelling is essential to supplement the measurements. (FILD is localized to the fixed poloidal position.)***

Feasibility of Alfvén eigenmode control using the EC-wave and the external 3D-field

- Alfven eigenmode control mechanism: Competition between the fast-ion drive and the wave-damping ($\gamma_{damping} > \gamma_{growth}$) → Increase the damping rate, or decrease the mode drive

Possible Control Tools:	NBI	ECH/ECCD	ICRH	3D-field
	Beam-ion profile change. → Change in drive	ECH changes slowing-down time profiles. → Change in drive	Change in fast-ion distribution and drive directly	Orbit stochastization → Change in drive
	Beam-ion damping, Sometimes contribute to thermal-ion Landau damping w/ high core T_i	Both ECH/ECCD are able to tailor the *q*-profile. → Change in Alfven continuum		Possible to modify the Alfven continuum

Demonstration of Alfvén eigenmode control using the ECCD for supporting high performance discharge

Experimental setup:

NBI heating (fast-ion drive), ECH, Co- & Counter-ECCD scan (q-profile tailoring)

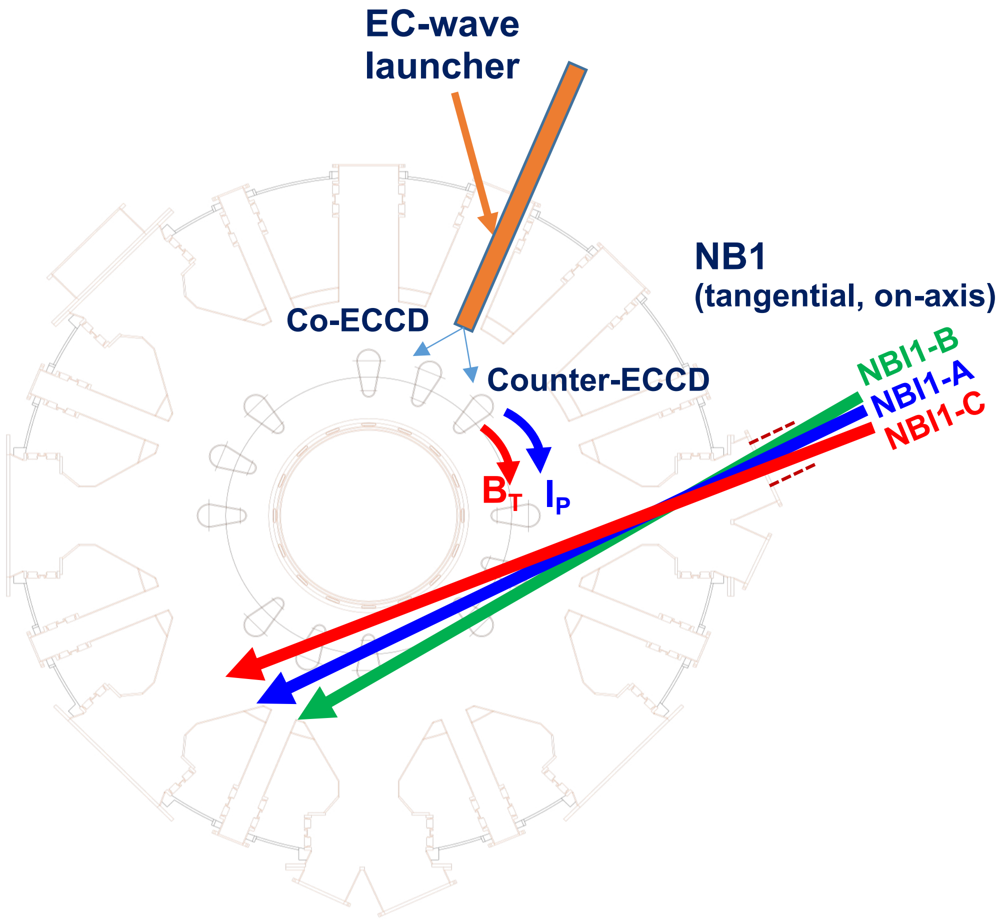

EC resonance layer (central ECH) movement by changing B_{T0}

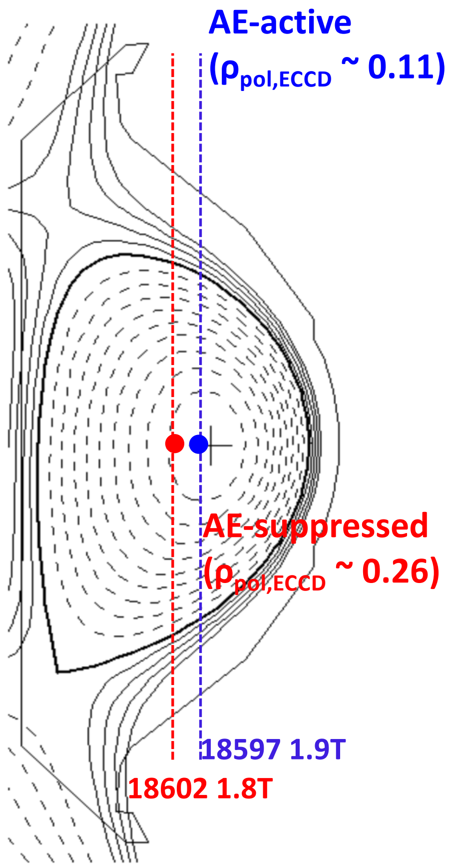

EC-wave mirror steering (on- & off-axis ECCD/ECH)

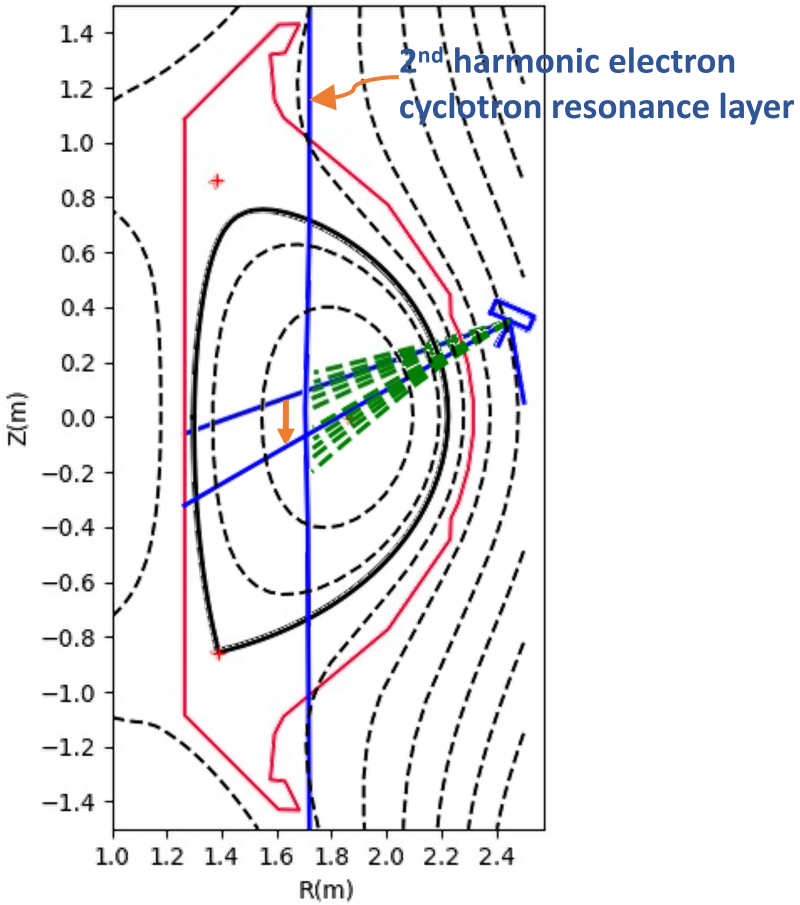

-20cm < $Z_{EC,target}$ < +20cm

-15° < ϕ_{EC} < +15°

Demonstration of Alfvén eigenmode control using the ECCD for supporting high performance discharge

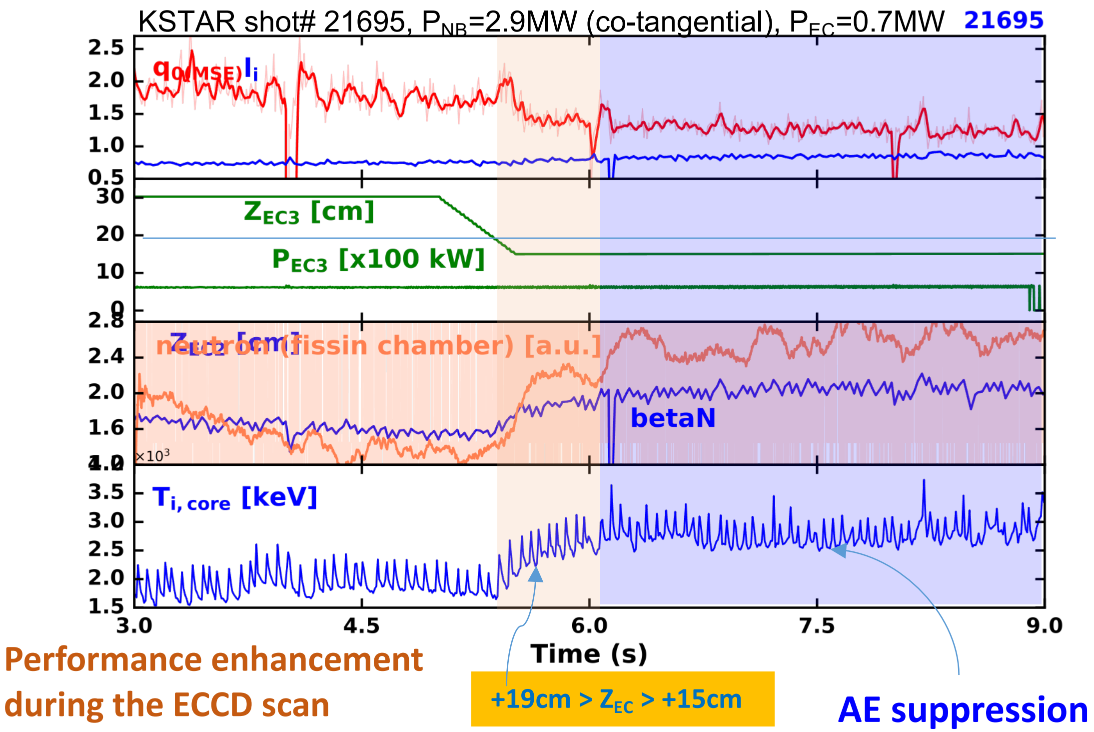

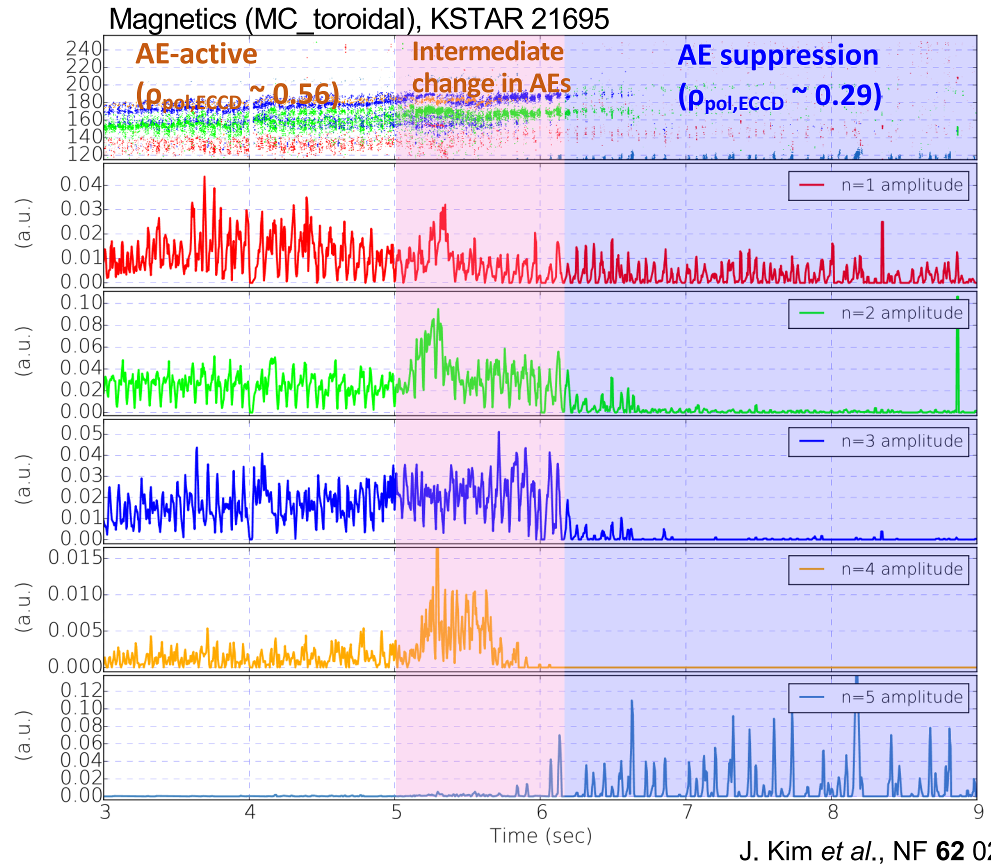

J. Kim *et al.*, NF **62** 026029 (2022)

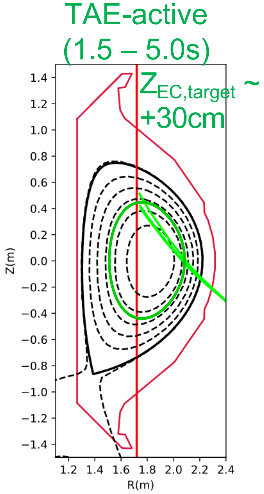

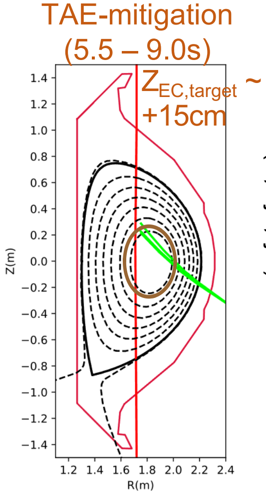

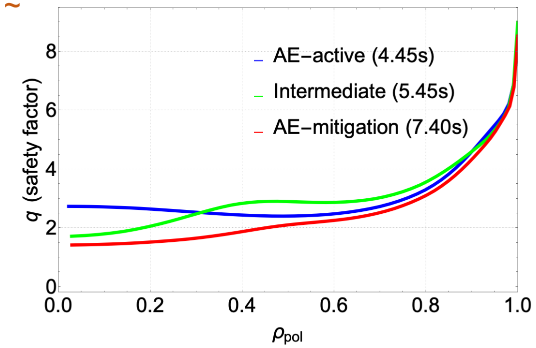

- **co-ECCD scanning found the TAE suppression by altering the central *q*-profile shape, increasing continuum damping in the elevated q_0 operation scenario. ➔**
- **Enhancement of performance (neutron rate, β_N, T_i, stored energy)**

Demonstration of Alfvén eigenmode control using the ECCD for supporting high performance discharge

P_{NB} ~ 3.4 MW (on-axis, co-NBI), P_{EC} ~ 1.3 MW
Co-ECCD, $\phi_{tor,EC}$ = +20°

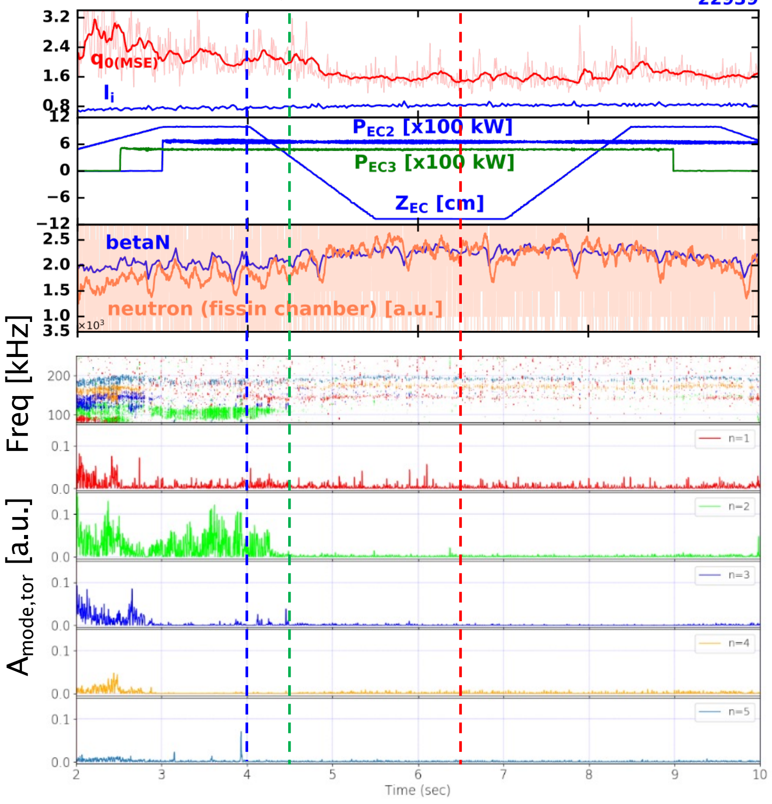

P_{NB} ~ 3.4 MW (on-axis, co-NBI), P_{EC} ~ 1.3 MW
Counter-ECCD, $\phi_{tor,EC}$ = −20°

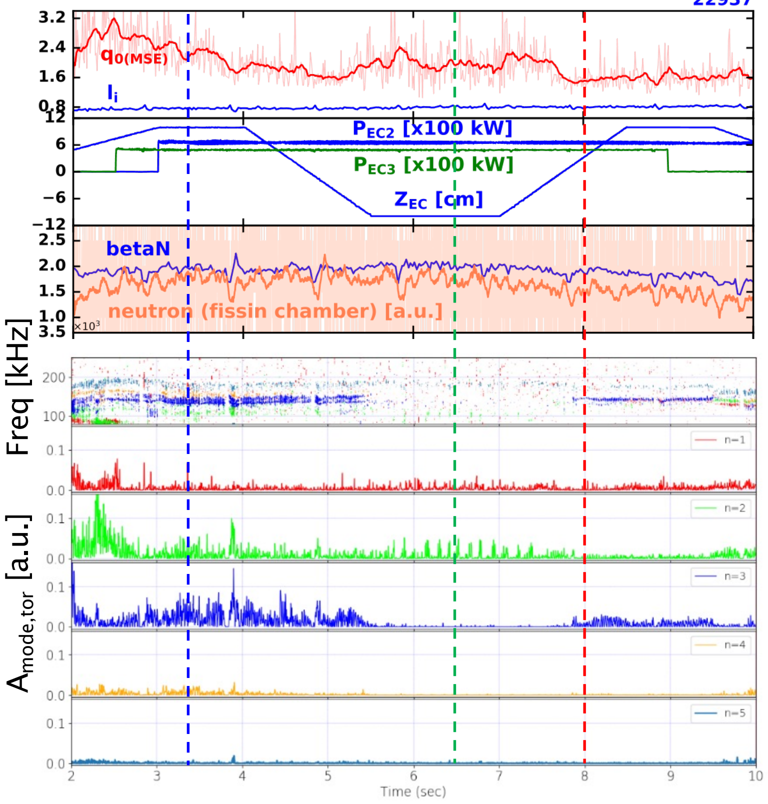

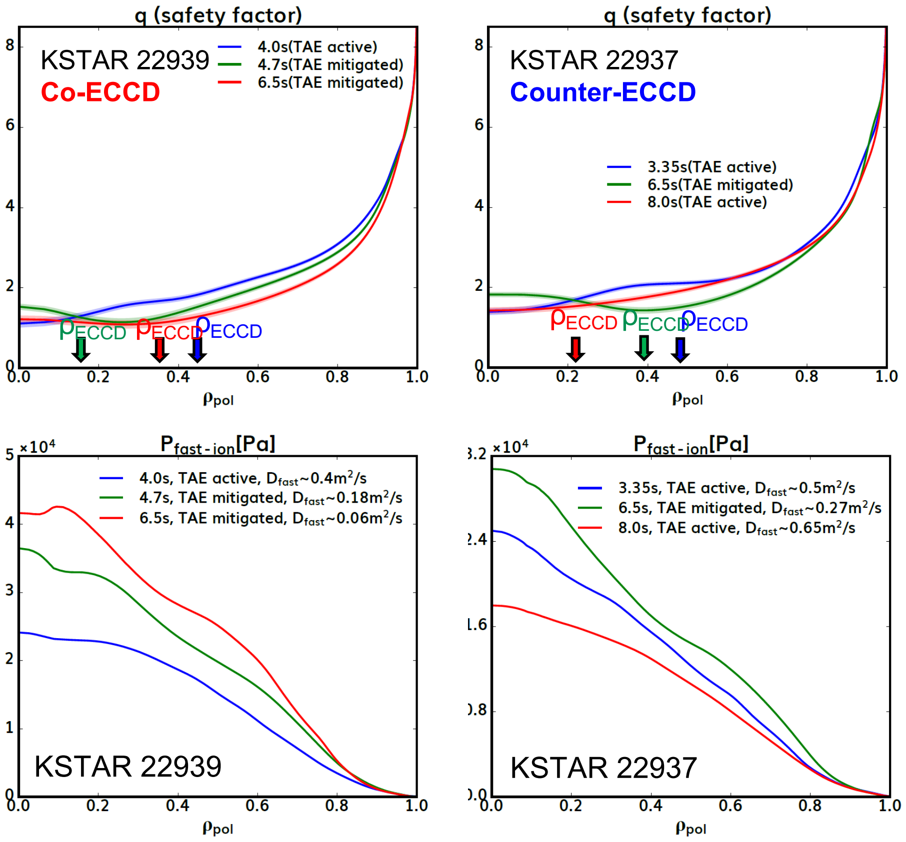

- **Both co- & counter-ECCD applications can mitigate or suppress the TAEs in elevated q_0 scenarios.**
- **Counter-ECCD application is beneficial to sustain a high q_0 scenario along with TAE mitigation. However, performance enhancement is limited.**

J. Kim *et al.*, IAEA FEC (2020)

Demonstration of Alfvén eigenmode control using the ECCD for supporting high performance discharge

21695, TAE-active stage (t ~ 4.45s)

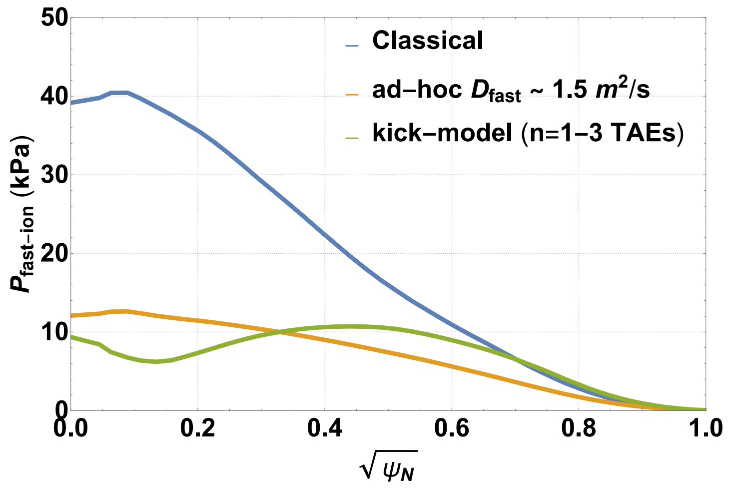

21695, TAE-suppression stage (t ~ 7.4s)

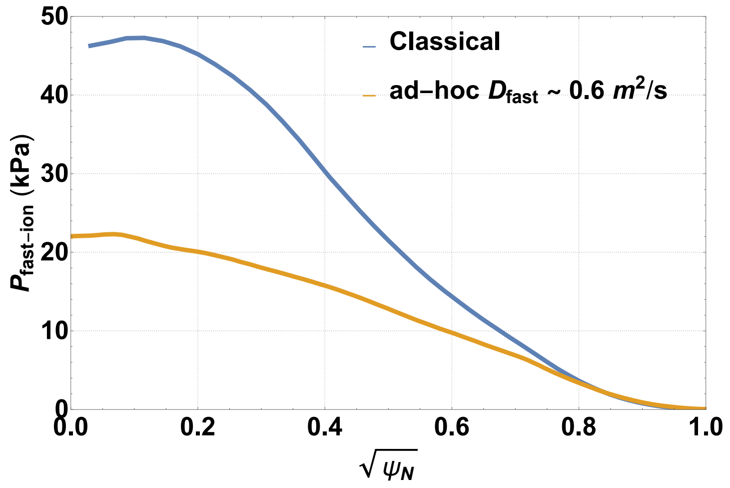

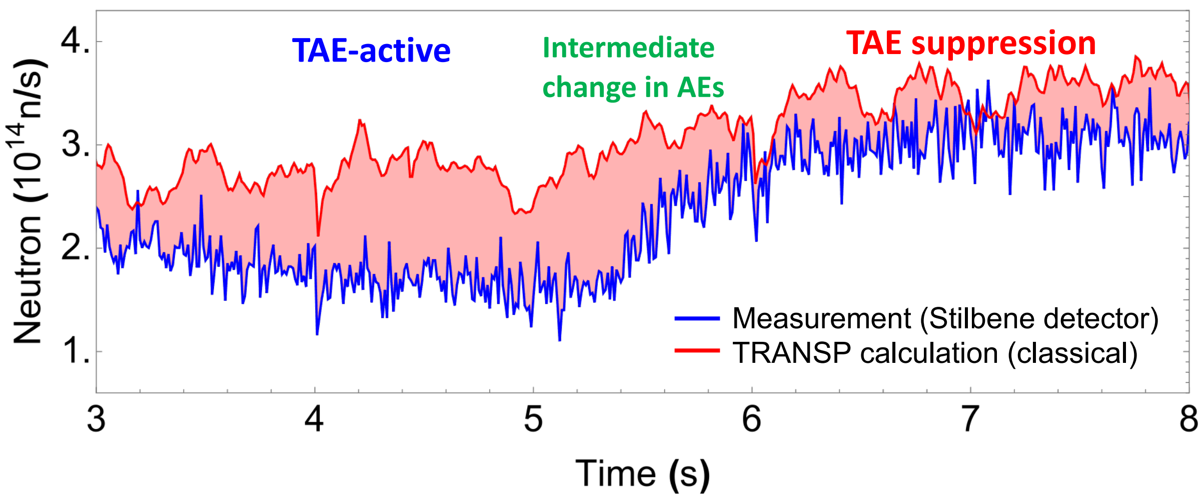

- Fast-ion pressure profiles (TRANSP) calculated and matched to the measured neutron emission rate → Reduced ad-hoc D_{fast} in the TAE-mitigation/suppression period

- Increase in central ion temperature in the TAE-suppression period

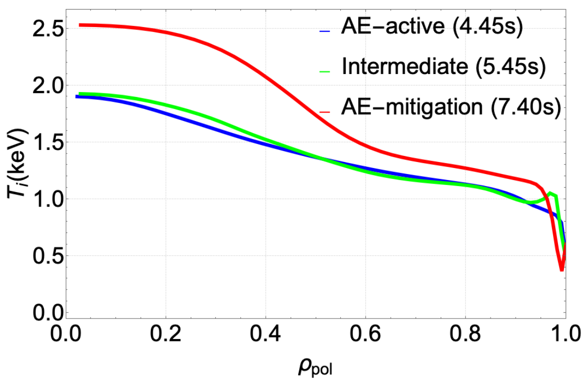

Demonstration of Alfvén eigenmode control using the ECCD for supporting high performance discharge

Fast-ion loss

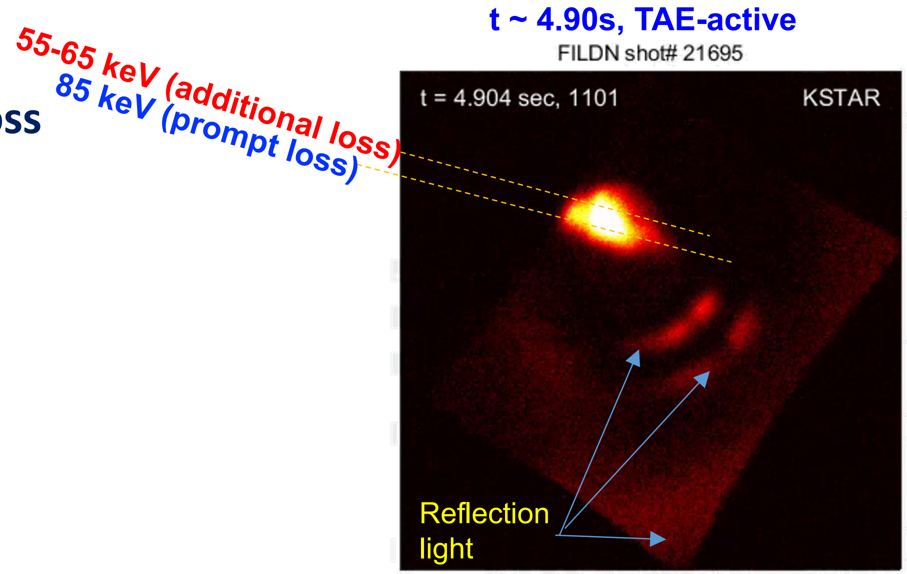

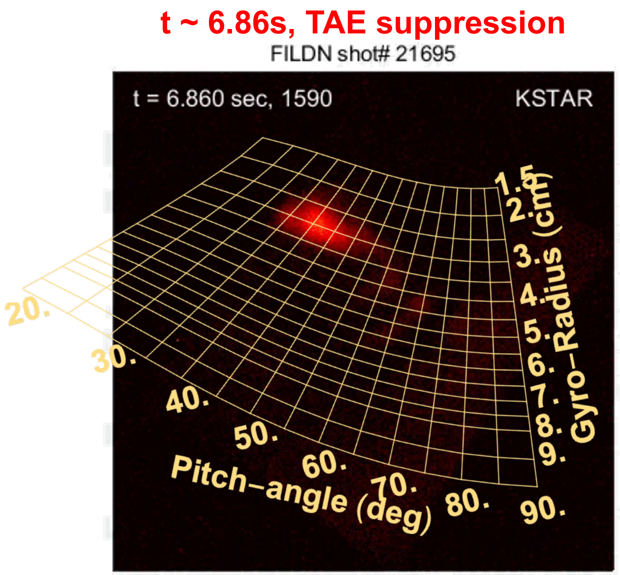

Possible cause of the additional losses (e.g. 65 keV beam-ion):

Interaction with *n*=3 TAE (modelled by 'Kick' model* w/ ORBIT & NOVA-K)

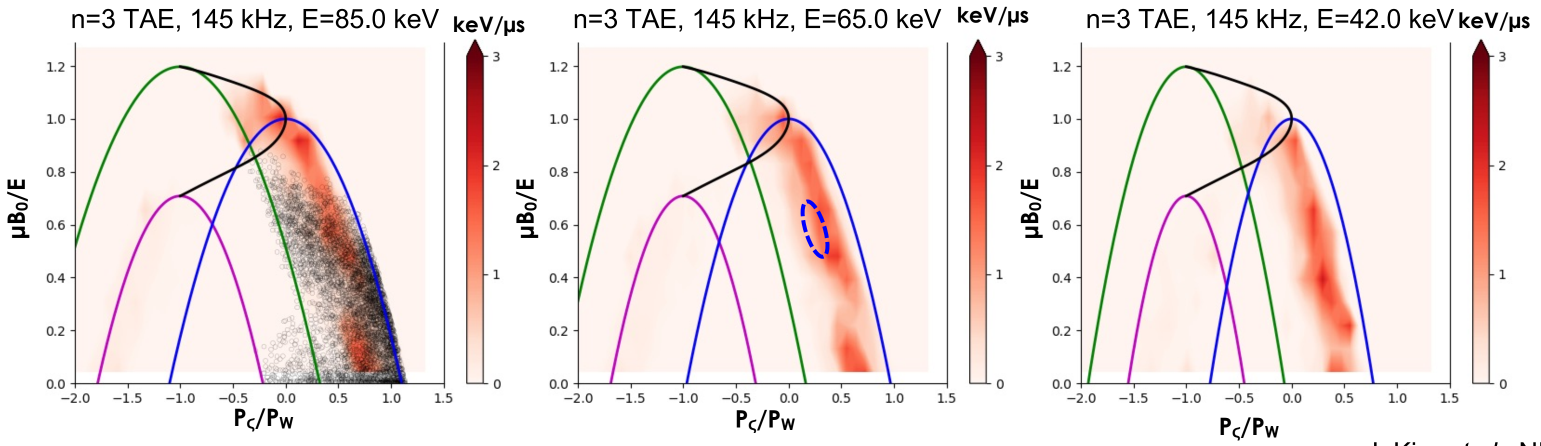

J. Kim *et al.*, NF **62** 026029 (2022)
*M. Podesta *et al.*, 2017 PPCF

Alfvén eigenmode control feasibility using the 3-D field

TAE control feasibility by scanning 3-D field phase window (K. Kim)

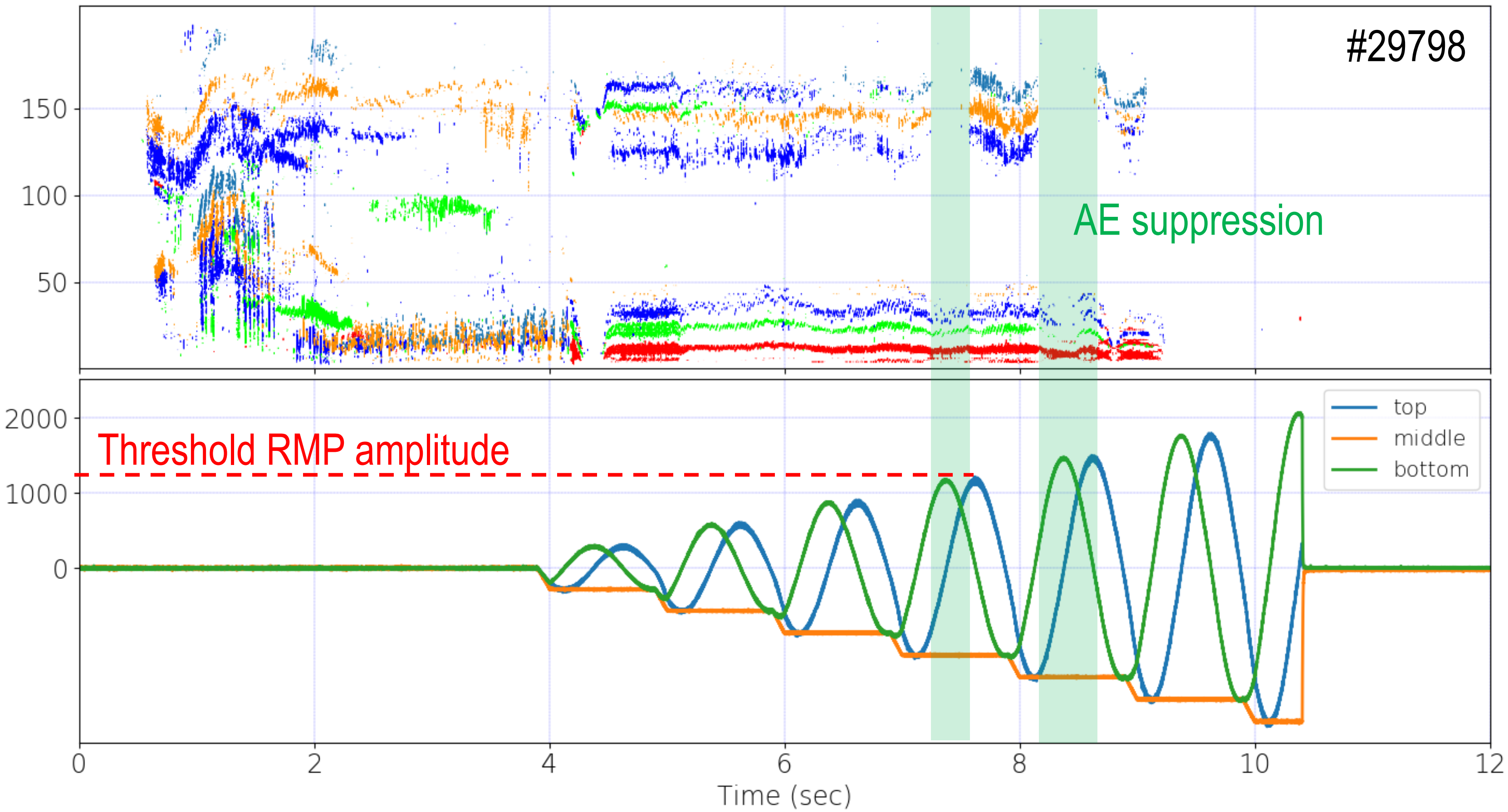

K. Kim et al., ITPA EP (2021)

- **Suppression of AEs by resonant 3D field phase achieved with threshold 3D field amplitude.**
  - A series of discharges show the same plasma response in the AE stability
  - ***3D-field phase window for AE suppression*** is identified → Largely resonant to the 3D field

Alfvén eigenmode control feasibility using the 3-D field

Plasmas kinetically respond to the 3D field and AE stability modification (K. Kim)

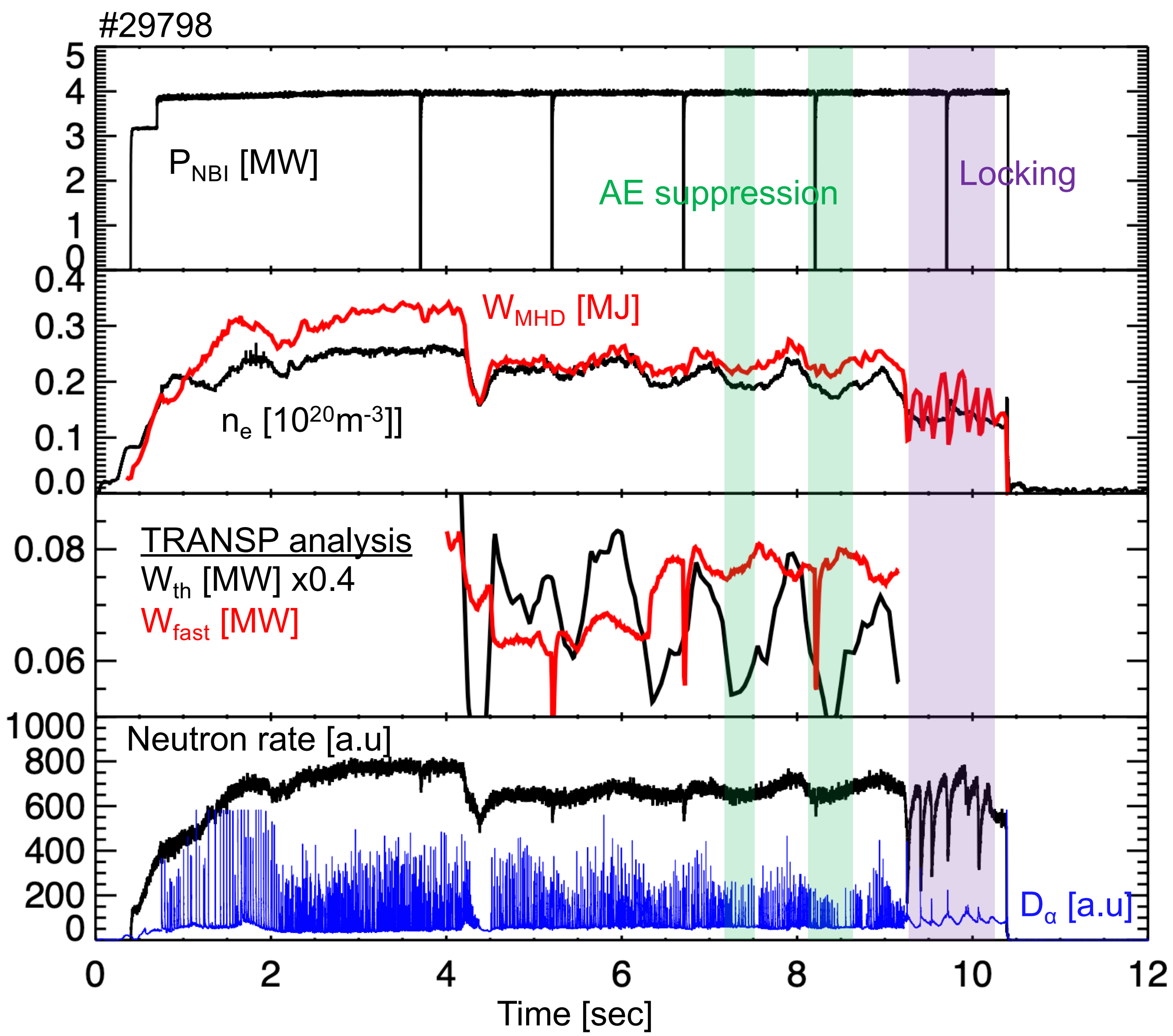

- **Plasma responses in the AE-suppressed phase are resonant:**
  - ✓ Density pump-out, stored energy decrease
  - ✓ 3D phase window for AE suppression is overlapped with ELM mitigation.
  - ✓ 3D field threshold for AE suppression is slightly weaker than the locking threshold → Amplitude window is narrow.

- **TRANSP analysis indicates:**
  - ✓ Fast ion stored energy is increased or (at least) sustained in the AE-suppressed phase.
  - ✓ Increased fast ion stored energy in the AE-suppressed phase compensates for degradation by resonant plasma response.

K. Kim et al., ITPA EP (2021)

Feasibility of Alfvén eigenmode control using the EC-wave and the external 3D-field

- Control of Alfvén eigenmodes (AE) has been performed by ECH/ECCD, 3D-field applications in KSTAR high β_P & high q_0 operation scenarios.
- Mainly co-I_P directional ECCD mitigates TAEs well. ➔ Performance enhancement (β ⇧, neutron ⇧, core T_e, T_i ⇧), but the on-axis or far off-axis ECCD/ECH is not effective.
- Major damping channel in the case of ECCD application is continuum damping.
- Enhancement of core T_i and plasma pressure (β) is also beneficial to suppress the TAEs.
- Suppression of AEs by resonant 3D field phase achieved with the threshold 3-D field amplitude and the proper phase.
- Plasma responses in the AE-suppressed phase are resonant.

Triton burnup study

Demonstration of alpha-particle confinement in current D-D fusion devices

- Two branches in D-D fusion reaction

  d + d → $_3$He (0.82 MeV) + n (2.45 MeV) 50%

  → **t** (1.0 MeV) + p (3.0 MeV) 50%

- **Triton burnup**

  d + **t** → $_4$He (3.5 MeV) + n (14.1 MeV)

Triton burnup ratio (TBR) = $\frac{Y_{n-dt}}{Y_{n-dd}}$

- **Due to the large width of the fusion-born triton, high I_P (i.e. mega-ampere) discharge w/ P_{NB} > 4 MW is preferred.**
- **Max. TBR is ~ 0.5% for I_P ~ 0.8 MA.**
- At higher I_P, TBR tends to decrease due to low-*f* MHD activities.

Plasma Current (MA)	1 MeV triton prompt loss fraction (%)
0.4	86.8
0.6	57.2
0.83	42.5
1.0	26.9

Triton burn-up ratio increases as plasma current increases. (*orbit-squeezing*)

J. Jo *et al.*, RSI 87, 11D828 (2016)

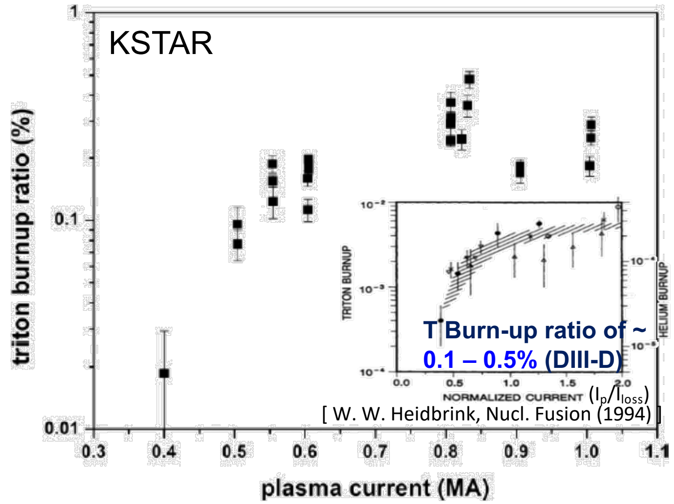

Triton burn-up dependence on *slowing-down* time $\propto \frac{T_e^{1.5}}{n_e}$

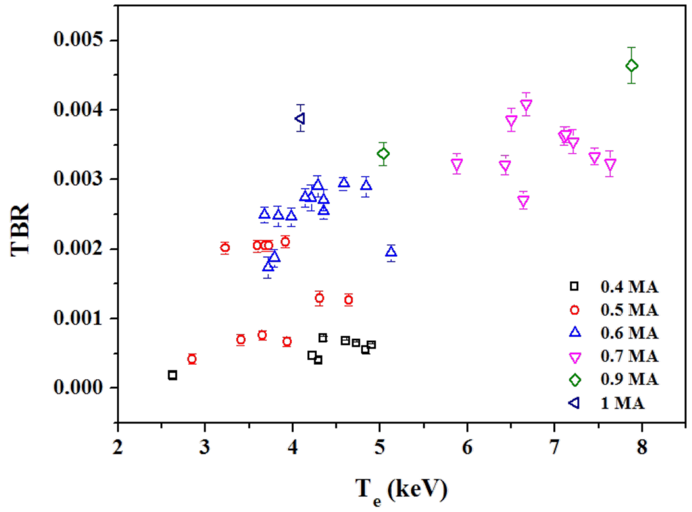

Triton burnup study

Demonstration of alpha-particle confinement in current D-D fusion devices

❖ Triton burnup is influenced by MHD activities.

Triton burnup decreases by MHD instabilities even in higher I_P.

I_P = 0.9 MA discharge

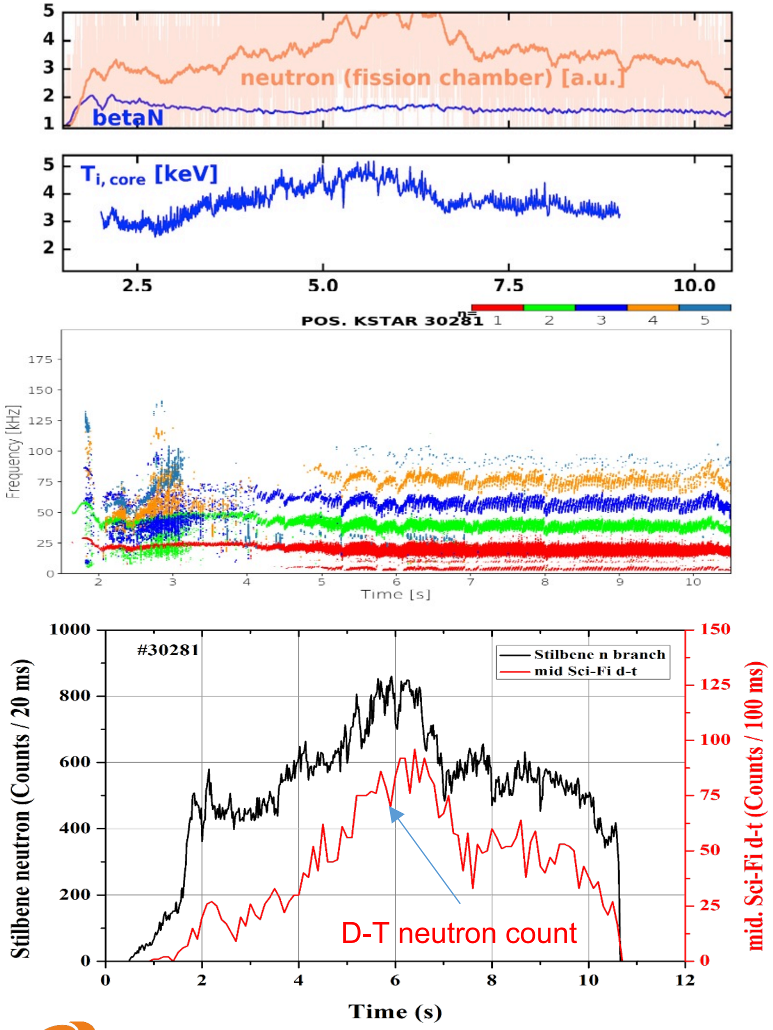

I_P = 0.8 MA discharge

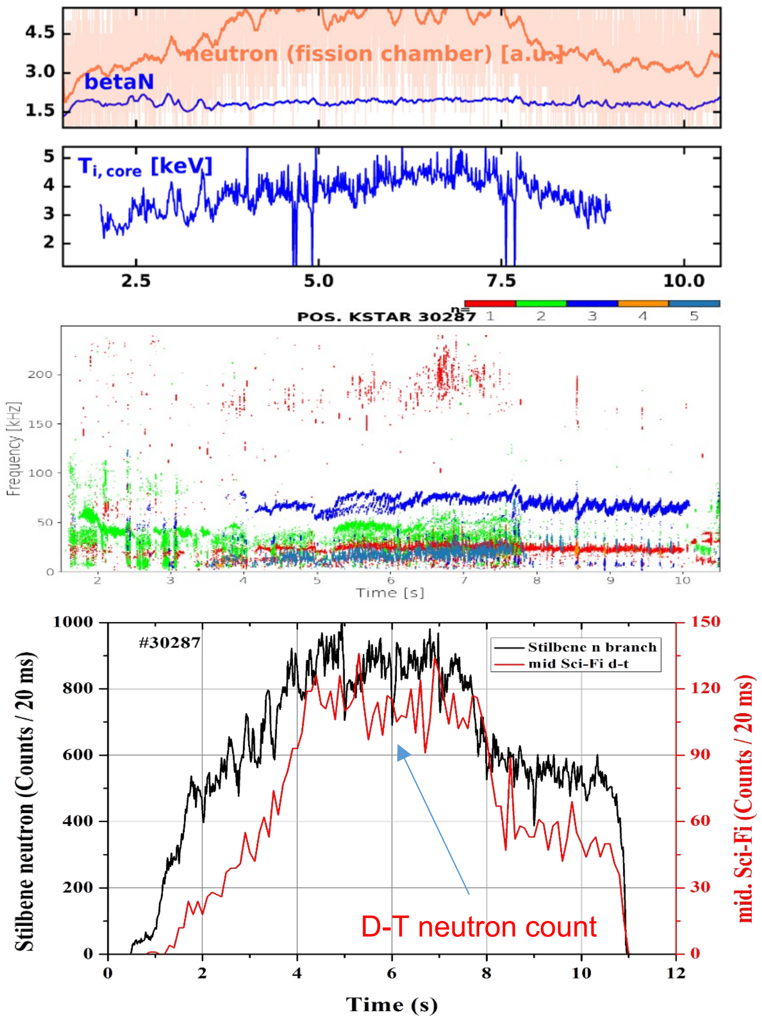

Triton burnup study

Demonstration of alpha-particle confinement in current D-D fusion devices

❖ 1 MeV triton confinement under the TAE control experiment

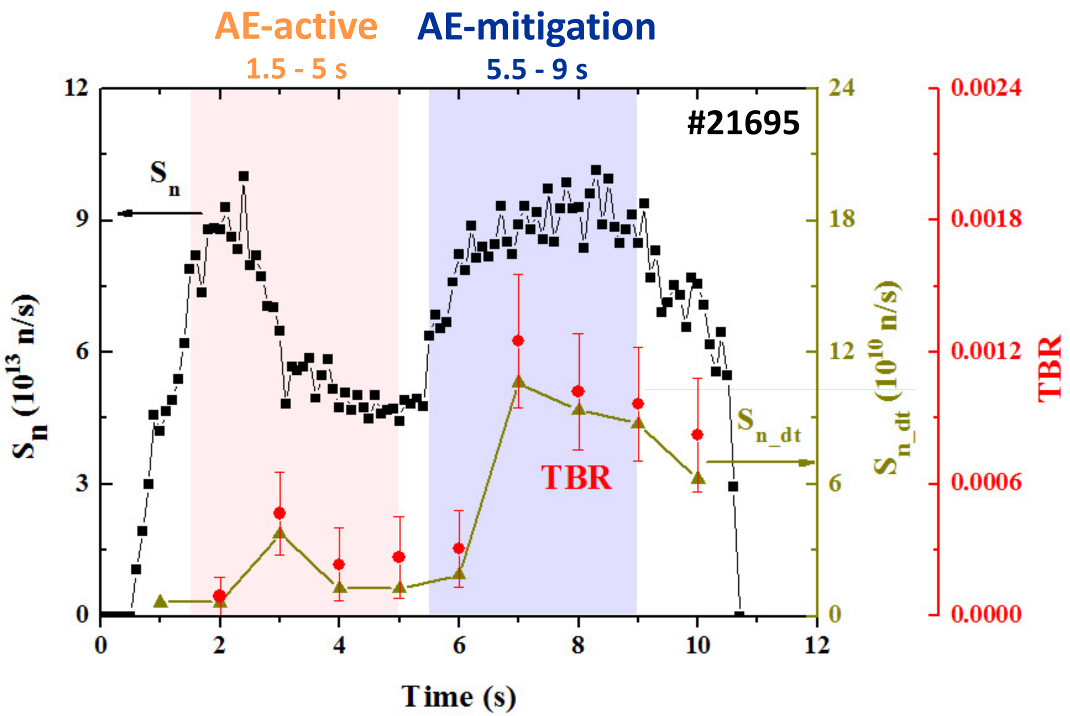

❖ Triton burnup simulation for data analyses

Orbit calculation: LORBIT

Burn-up calculation based on the classical theory

$$\Delta N = TBR_{classical\_cal.} - TBR_{measured}$$

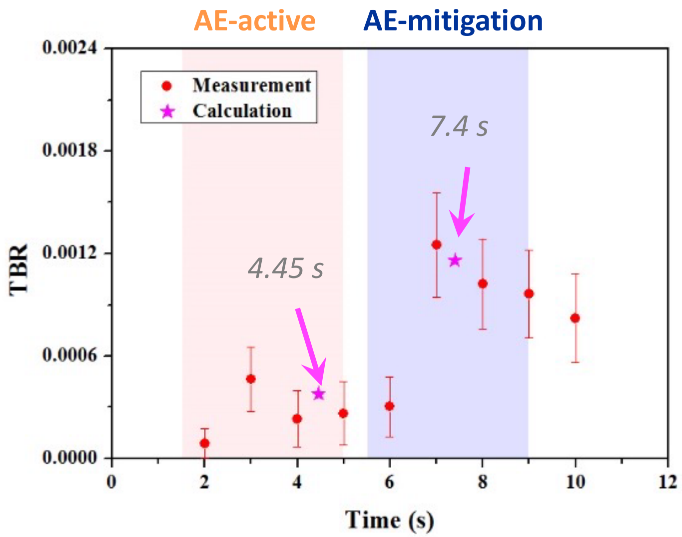

Triton burnup study
Summary

- Triton burnup experiment has been performed to demonstrate the dynamics of the fusion-born charged particles (i.e. α–particle) in the medium-size fusion devices.
- Reference discharge for this experiment is produced from the stable operation of mega-ampere discharges. (avoiding loss of fast-triton due to large orbit-width)
- Triton burnup ratio increases as I_P and slowing-down time increase.
- Low-*n* core MHD activities (i.e. sawtooth crash, tearing mode) degrade the fast-triton confinement.

2. EP diagnostics on KSTAR

- Fast-ion loss detector
- Fast-ion charge-exchange spectroscopy
- Neutron diagnsotics

Fast Ion Loss Detector

Hardware set-up

- FILD Scintillator material : ZnS:Ag, YAP:Ce
- CMOS camera: 100 – 2000 fps
- PMT: 2 MS/s
- Nominal head position: R_{head} = 2.27 – 2.28m

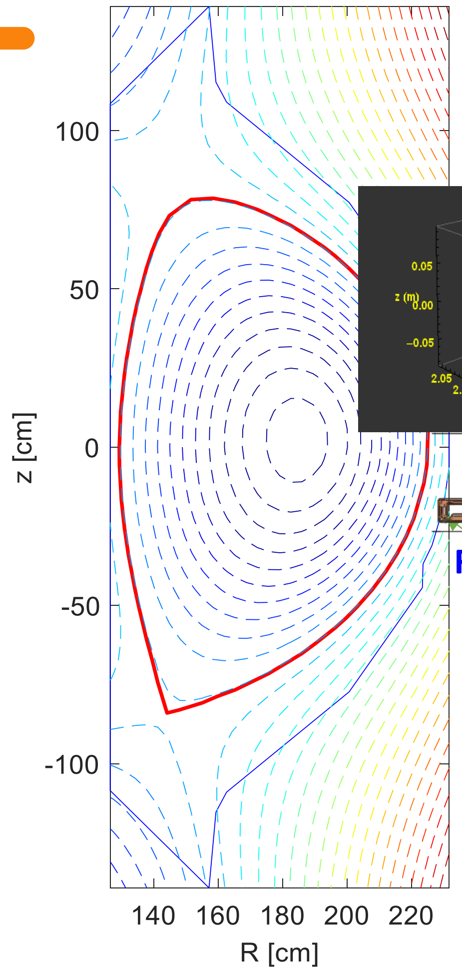

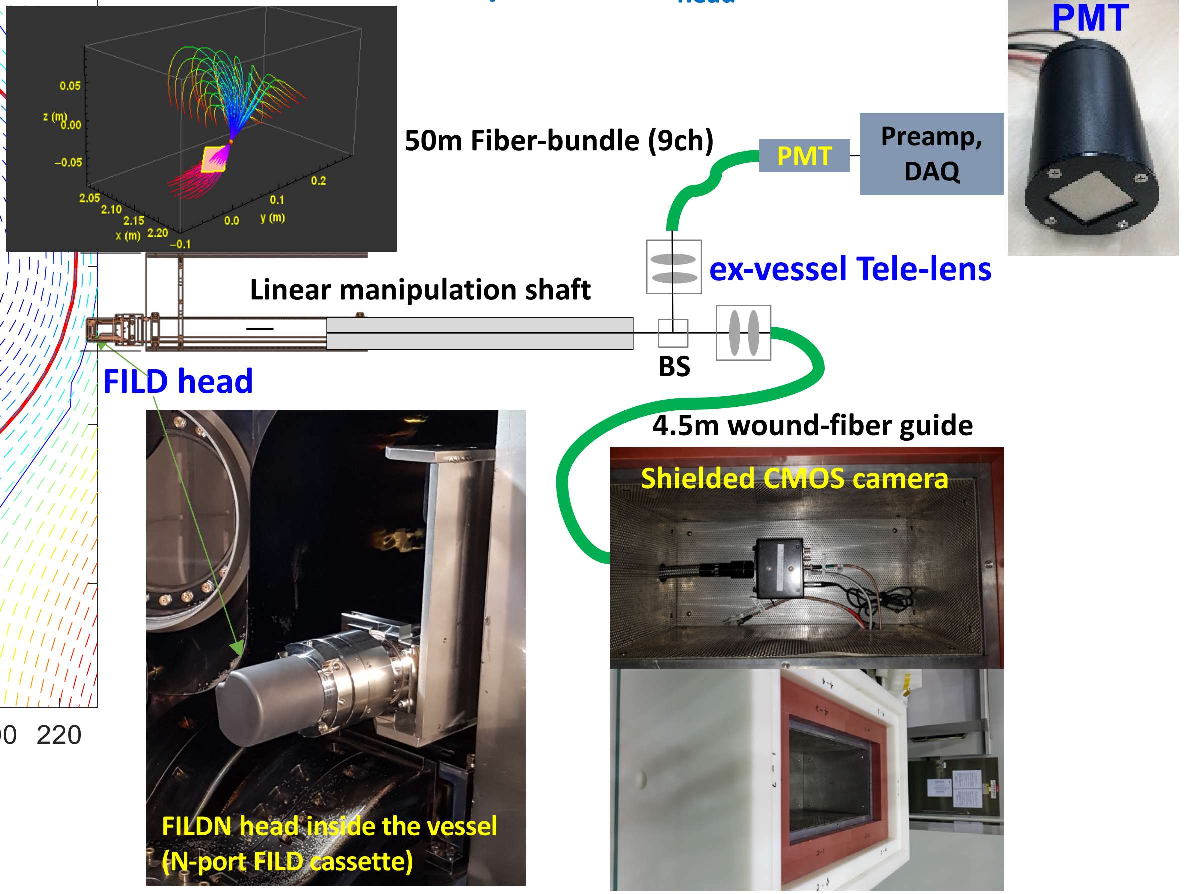

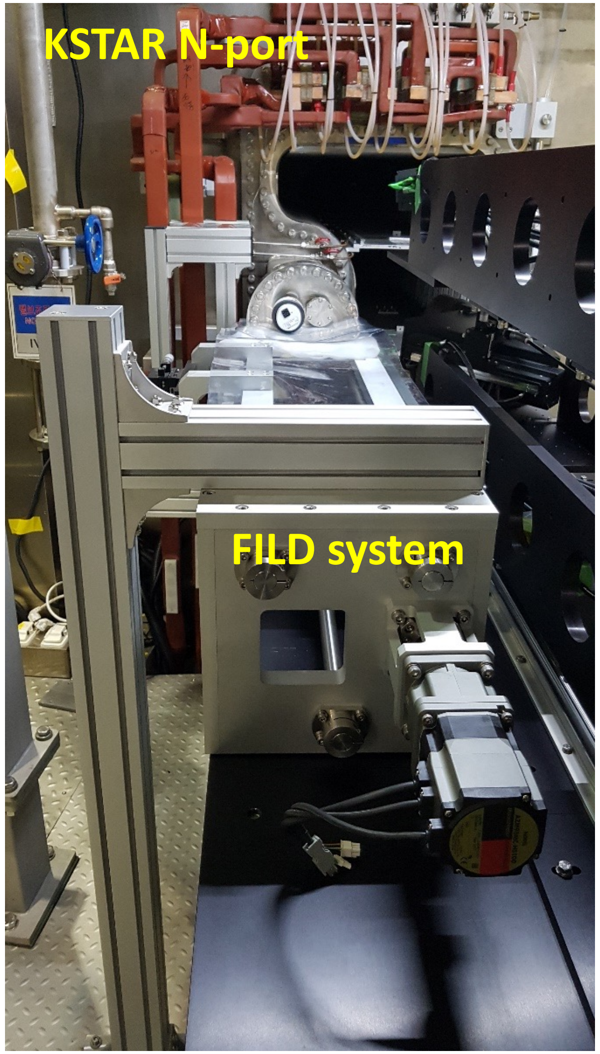

Fast Ion Loss Detector
Measurement examples

FILD CCD camera (200 fps):
Phase-space (scintillator map) of lost fast-ions in the 3-D field ELM control experiments

FILD PMT (2 MS/s):
Fast measurement of transient fast-ion losses associated with the beam-ion-driven EPMs

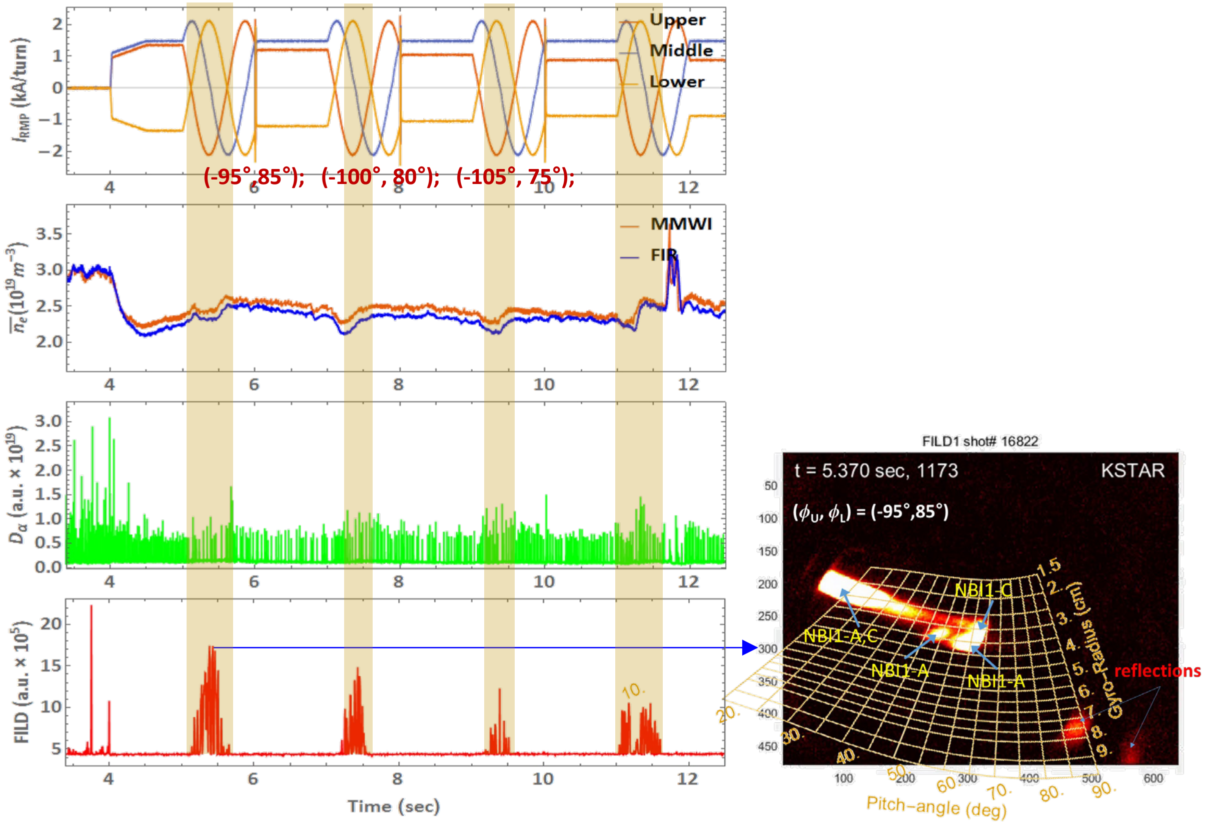

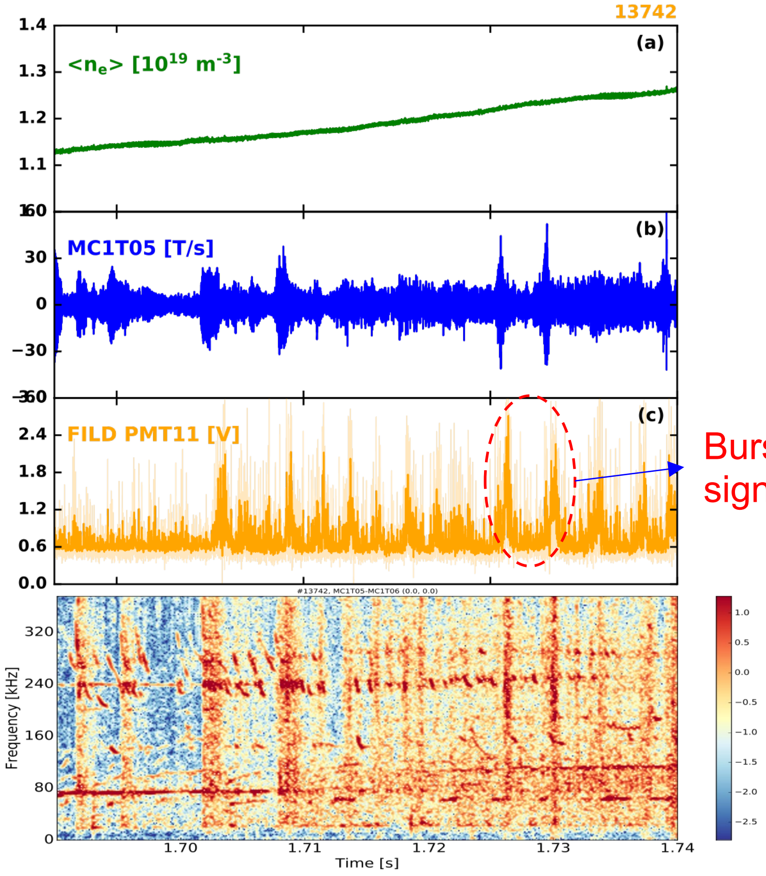

Bursts of fast-ion loss signal (FILD PMT)

Fast Ion Loss Detector

near-term Plan

- **Re-calculation of fast-ion load on the N-port FILD-head**
  - Weaker fast-ion loss intensity at the N-port → Recheck the suitability of the current FILD location through full-orbit simulations
- **Reversed B_T**
  - Fast-ion loss in the advanced operation scenario with reversed B_T direction
  - Optimization of FILD-head orientation and shape
- **Upgrade of measurement system**
  - Check the camera optics
  - DAQ upgrade (2MS/s/ch), PMT electronics w/ new pre-amplifiers

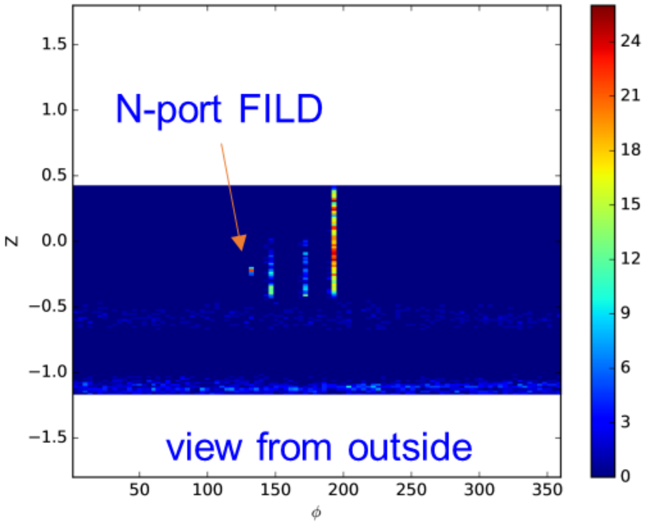

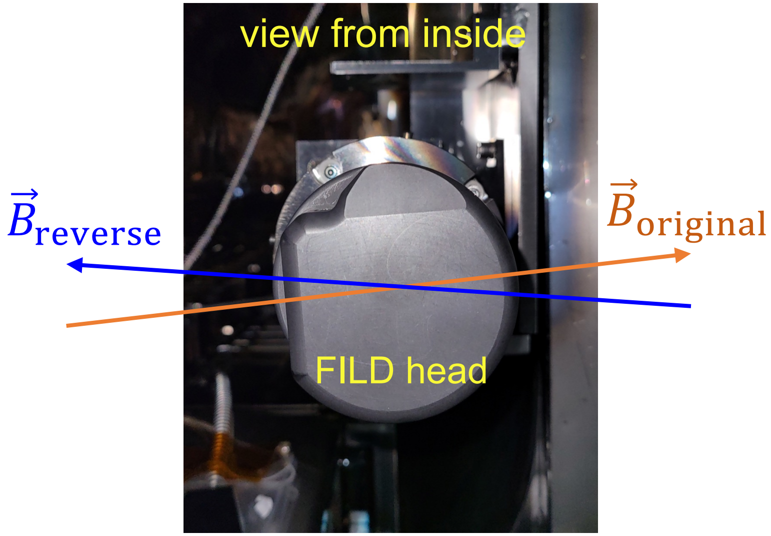

FIDA (Fast Ion D_α) Spectroscopy

Layout, Specification

J.W. Yoo *et al.*, RSI **92**, 043504 (2021)
M.H. Kim *et al.*, HTPD 2022

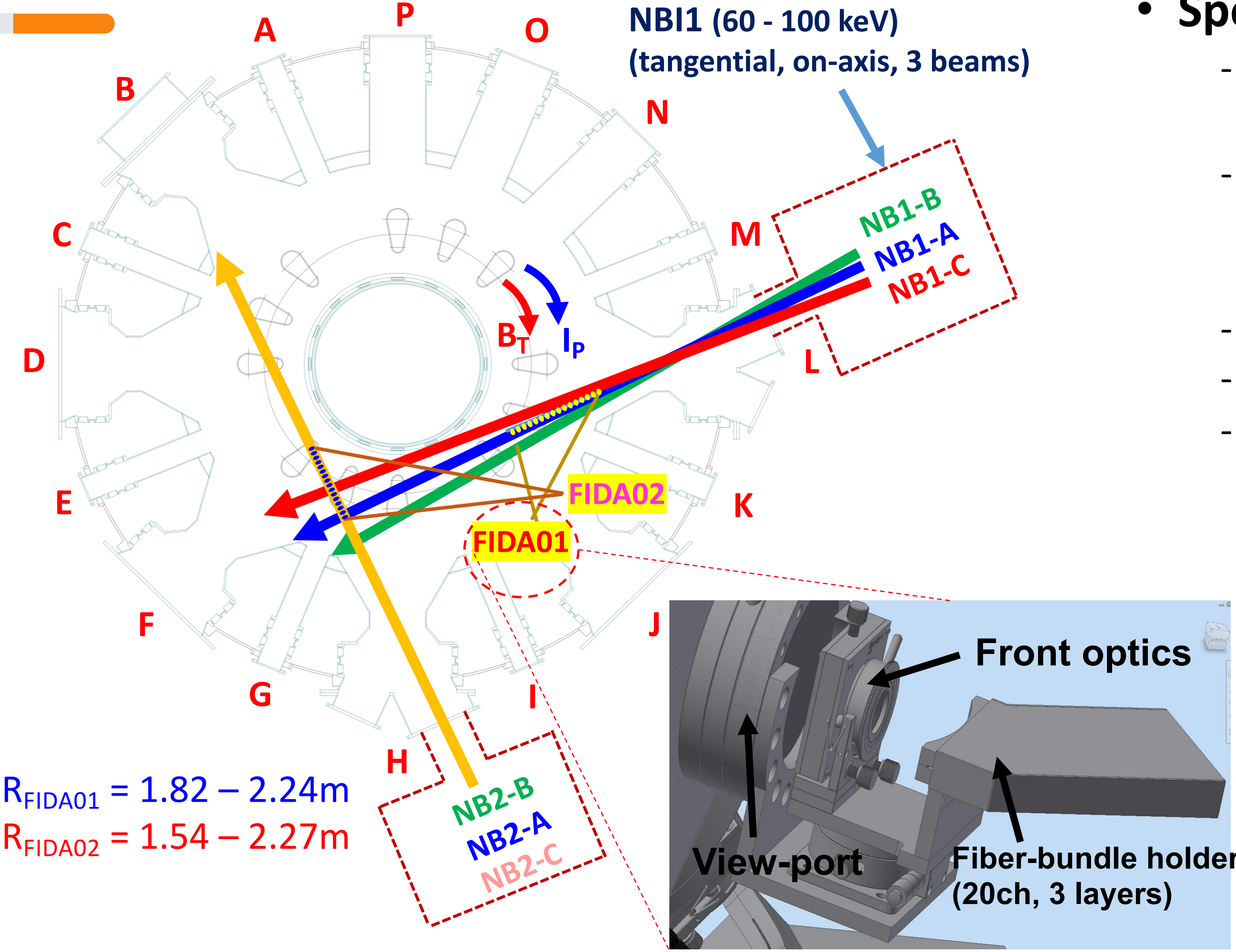

R_{FIDA01} = 1.82 – 2.24m
R_{FIDA02} = 1.54 – 2.27m

- **Specification:**
  - **FIDA01 (16 ch)**
    - **Blue-shifted** FIDA emissions of **NB1A** source
  - **FIDA02 (10 ch)**
    - **Red-shifted** FIDA emissions of **NB2A** source
  - Radial resolution : ~ 2 cm (FIDA01) / ~5 cm (FIDA02)
  - Frame rate: 100 Hz (typ.)
  - Exposure time: ~2 ms (typ.)

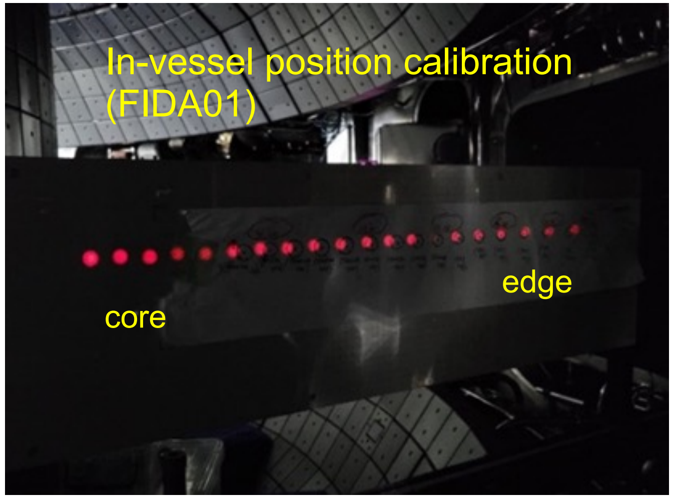

FIDA (Fast Ion D_α) Spectroscopy

Upgrade in 2021-2022 (SCT spectrograph, Filtered ultra-fast FIDA)

Schematic of Schmidt-Czerny-Turner (SCT) Spectrograph

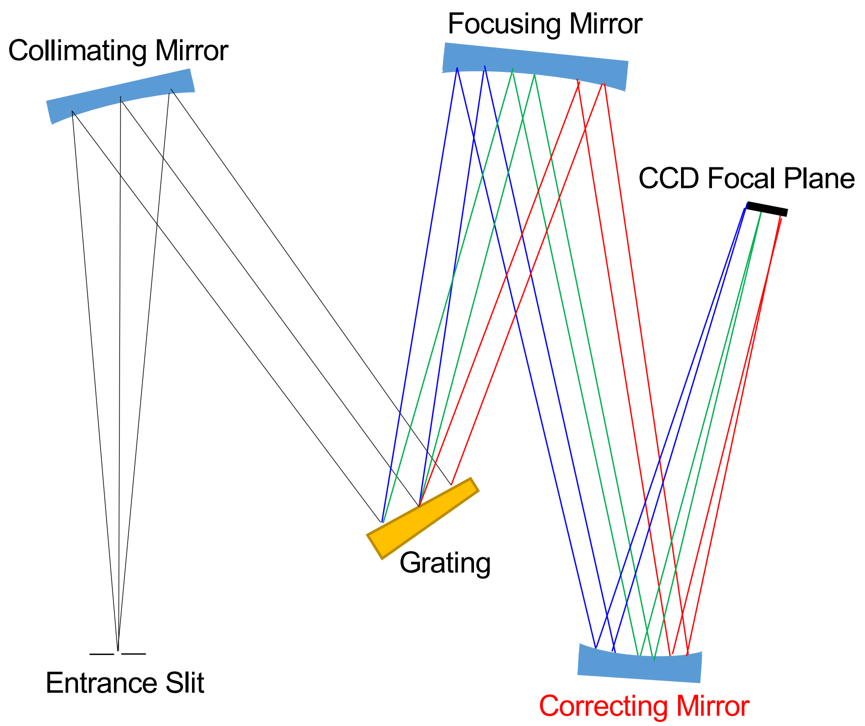

J.P. McClure et al., PISCES (Photonic Innovations and Solutions for Complex Environments and Systems) II; 91980C (2014)

Test images (CCD):

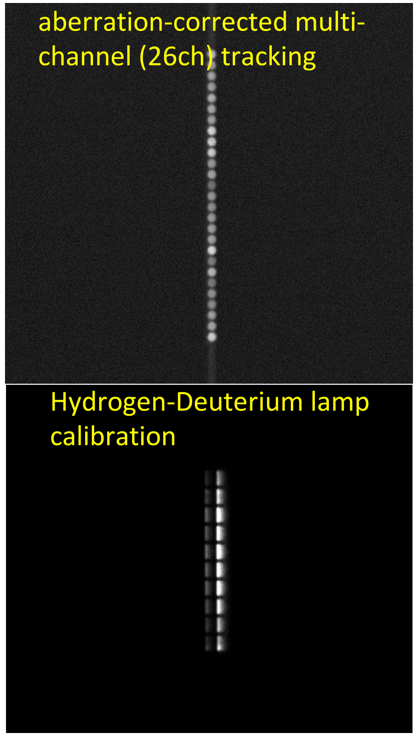

Almost no aberration on the image plane

Schematic of Filtered ultra-fast FIDA system

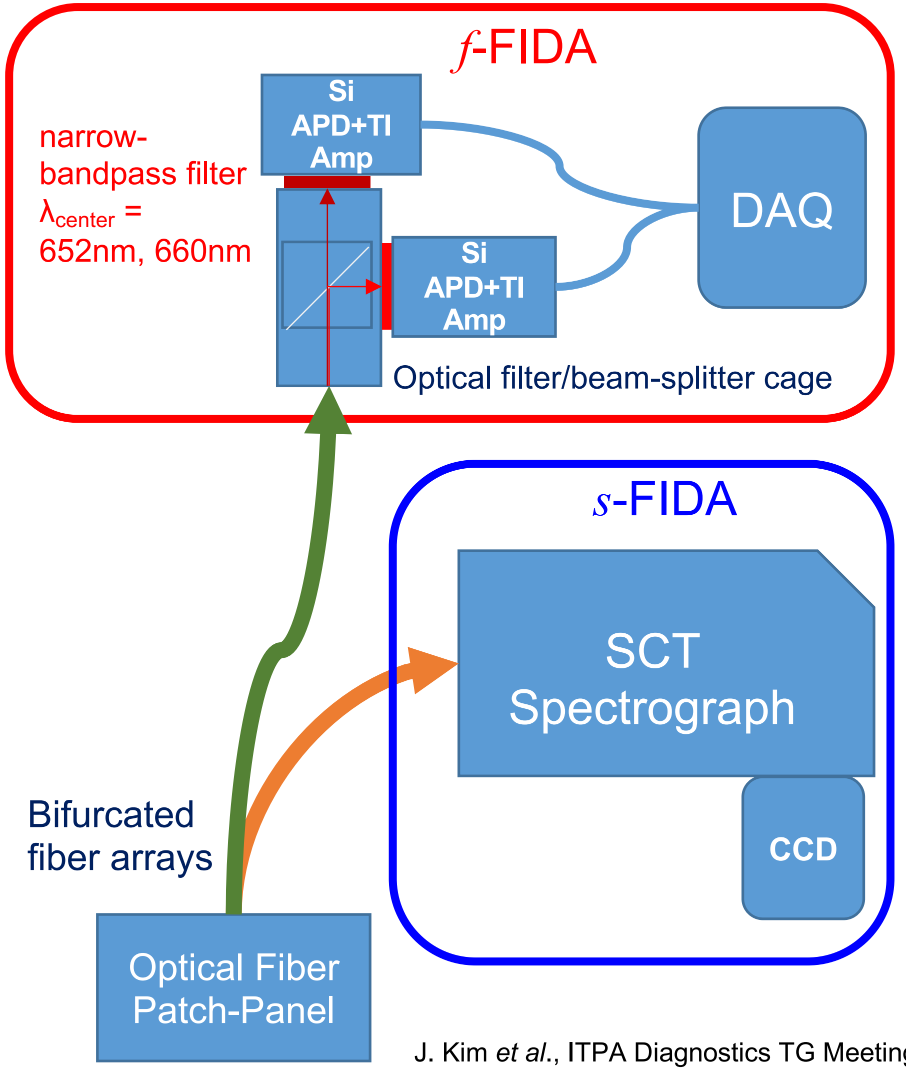

J. Kim *et al.*, ITPA Diagnostics TG Meeting (2021)

FIDA (Fast Ion D$_\alpha$) Spectroscopy
Measurement examples (FIDASIM calculation, FIDA intensity profile)

Measured Spectra (neutral-beam subtracted)

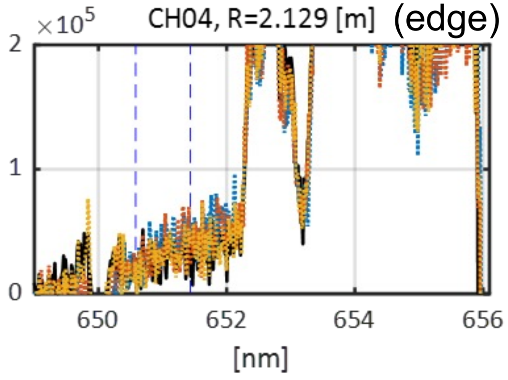

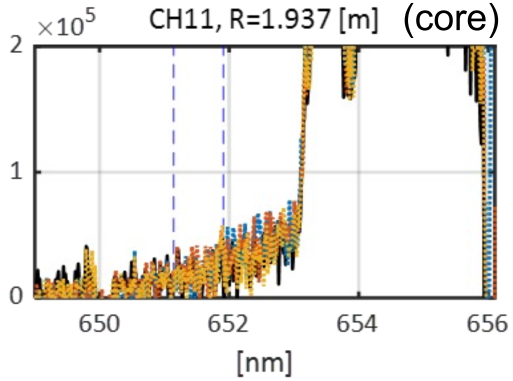

FIDASIM

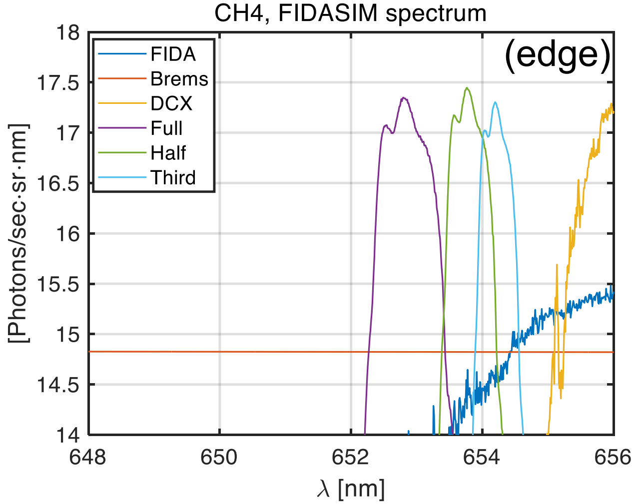

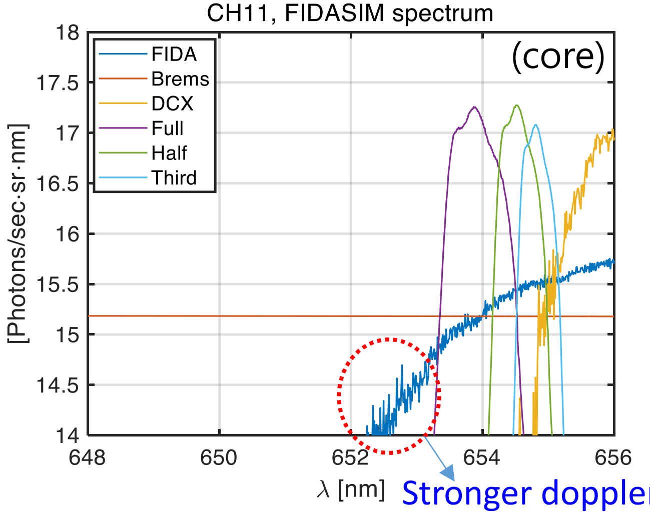

Stronger doppler-shift:
higher fast-ion energy

Measurement example
(fast-ion transport in the 3-D field experiment)

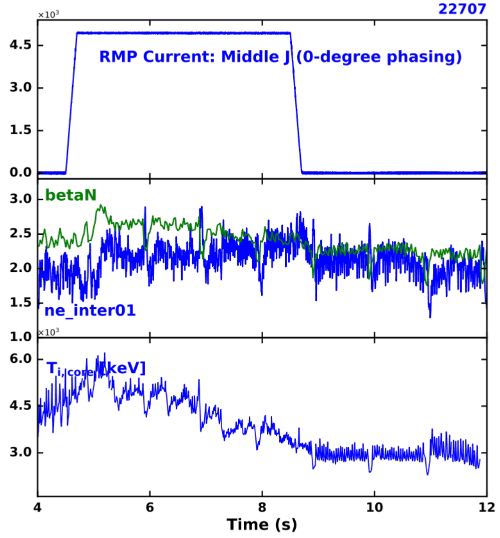

e.g. Single energy FIDA intensity profiles

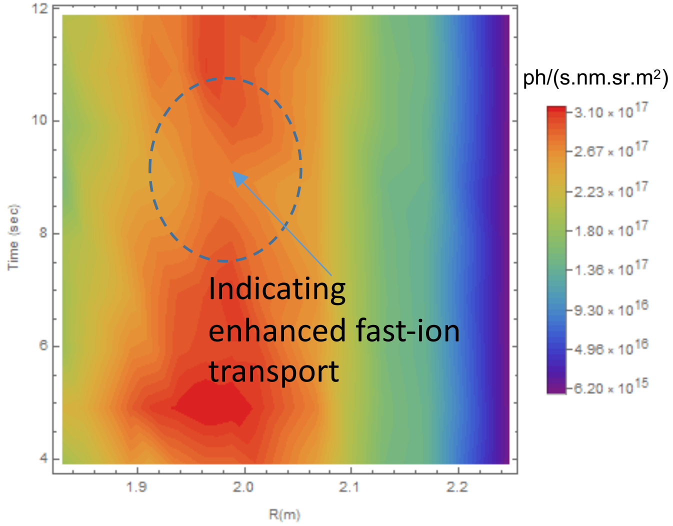

FIDA (Fast Ion D_α) Spectroscopy
near-term plan

- **Oblique-view FIDA to support *fast-ion velocity-space tomography***
  - **Oblique-view to NB1 (blue-shift), Preparation for 2023 campaign**
  - **Adopting the *fast-ion phase-space visualization* without modelling, combined with the tangential FIDA views**
  - ***Key challenge*: how to install the front-optics inside the small volume of the passive-plate structure → *Miniaturization*!**

- **Consideration of passive FIDA array (free of beam-blip?)**

FIDA weight function example (E = 50 – 70 keV)

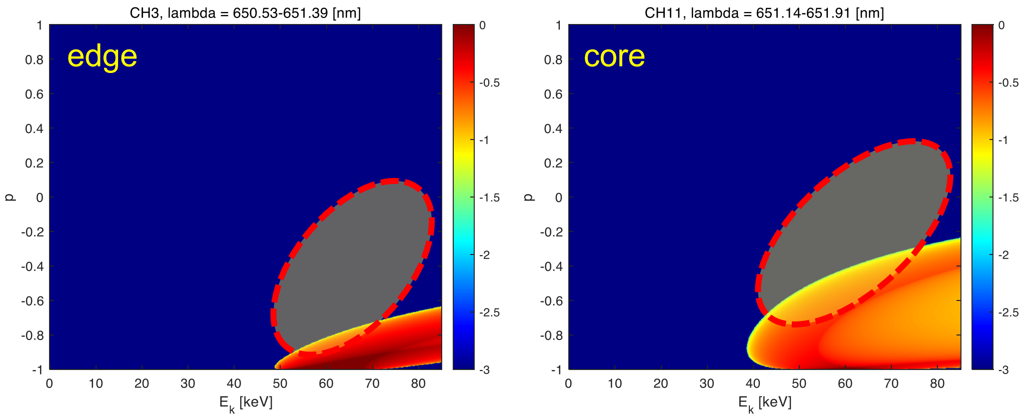

Additional oblique-views: *Extended phase-space coverage*

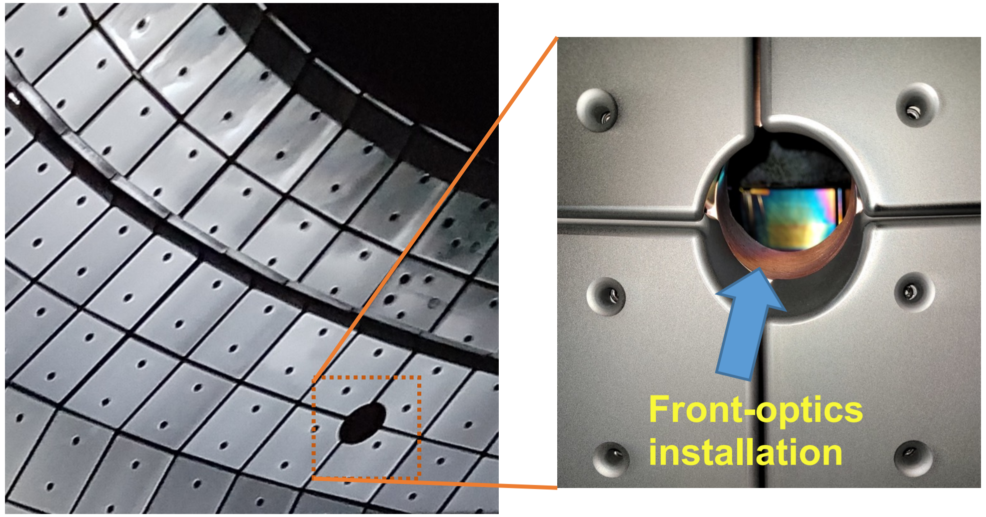

Scintillator-based Neutron Diagnostics

Organic scintillator (NE213, Stilbene) Detector

- **Scintillator (NE213, Stilbene)**
  - **To measure the D-D fusion neutron (2.45 MeV) rate**

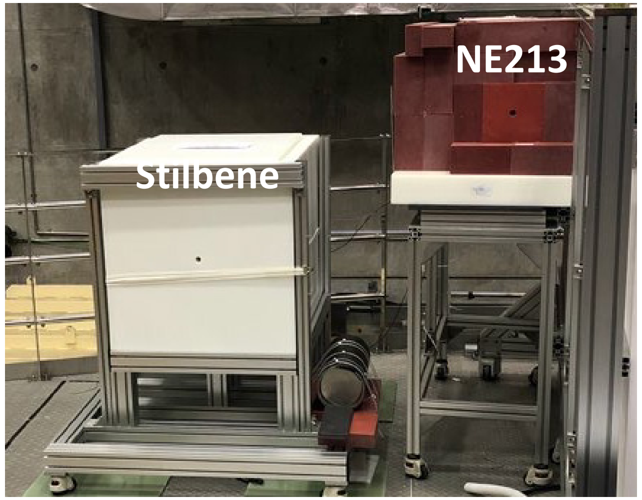

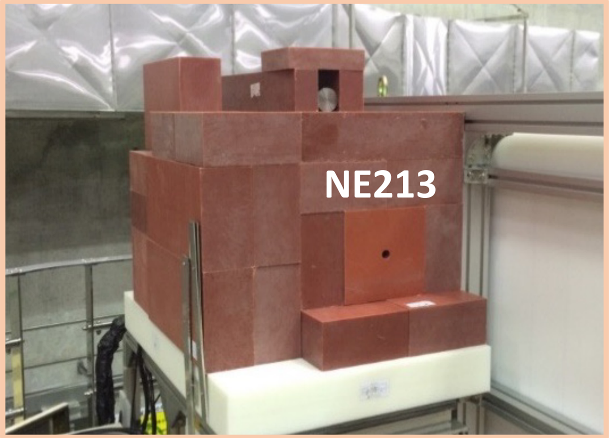

Scintillator

PMT detector

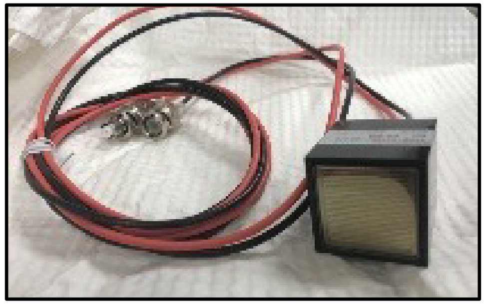

Magnetic shield

Neutron detector module

Pulse signal discrimination & count

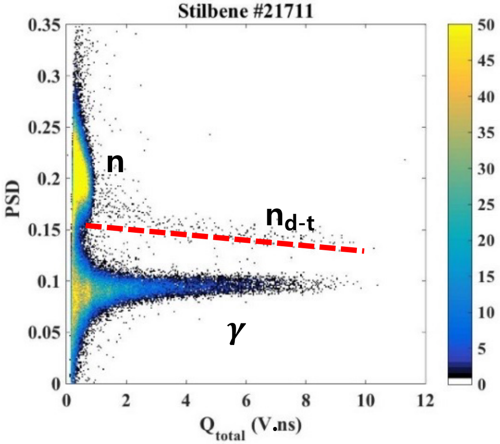

Effective pulse counts → neutron rate

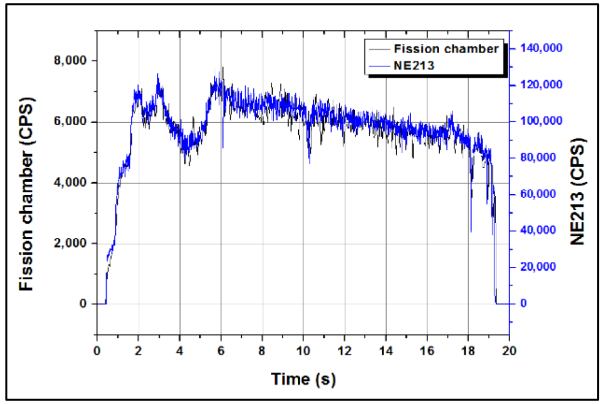

J. Jo *et al.*, RSI **89**, 0I118 (2018)
K. Ogawa *et al.*, RSI **89**, 10I101 (2018)
J. Jo *et al.*, RSI **87**, 11D828 (2016)

Scintillator-based Neutron Diagnostics

Scintillating-Fiber Detector for measuring D-T neutrons

➢ Scintillating fiber (a.k.a. Sci-Fi) detectors for 14 MeV D-T neutron measurements (many fibers inside the Aluminium mats)

- **Operation principle:** high pulse-height for measuring axially incident D-T neutrons
- Pulse height: n_{DT} discrimination
- Application to the triton (fusion-born) burnup study

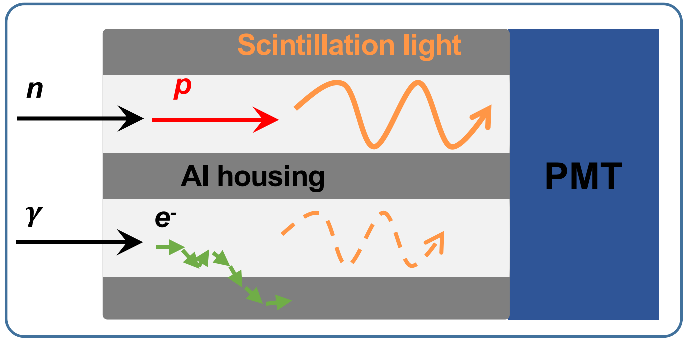

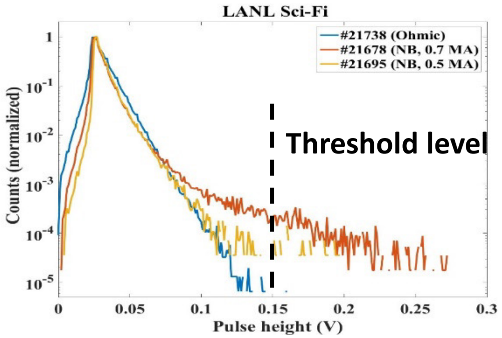

Small size

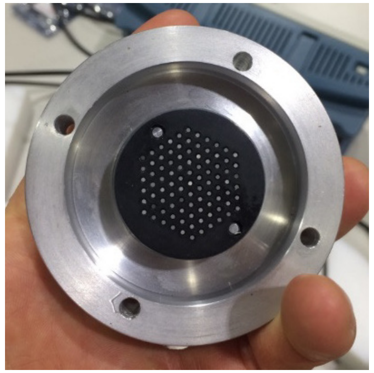

ϕ = 1 mm, 91 fibers

Mid. size

2-inch Φ

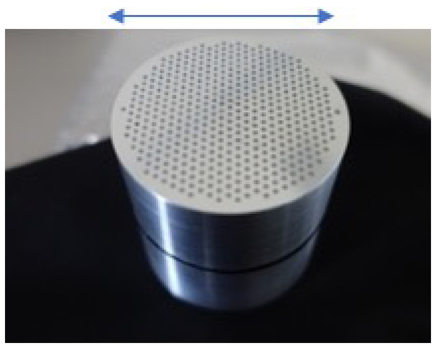

ϕ = 1 mm, 456 fibers

Large size

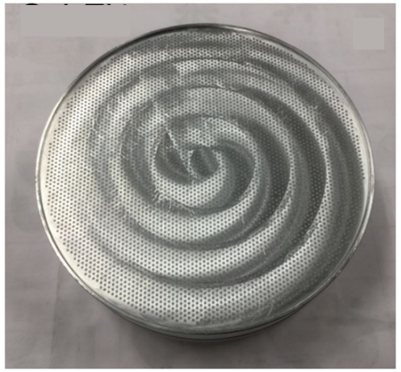

ϕ = 1 mm, 5156 fibers

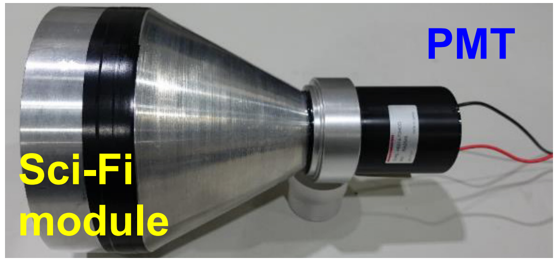

NAS (Neutron Activation System)
ITER Prototype

M.S. Cheon *et al.*, J. Instrum. **7** (05), 2012

ITER NAS

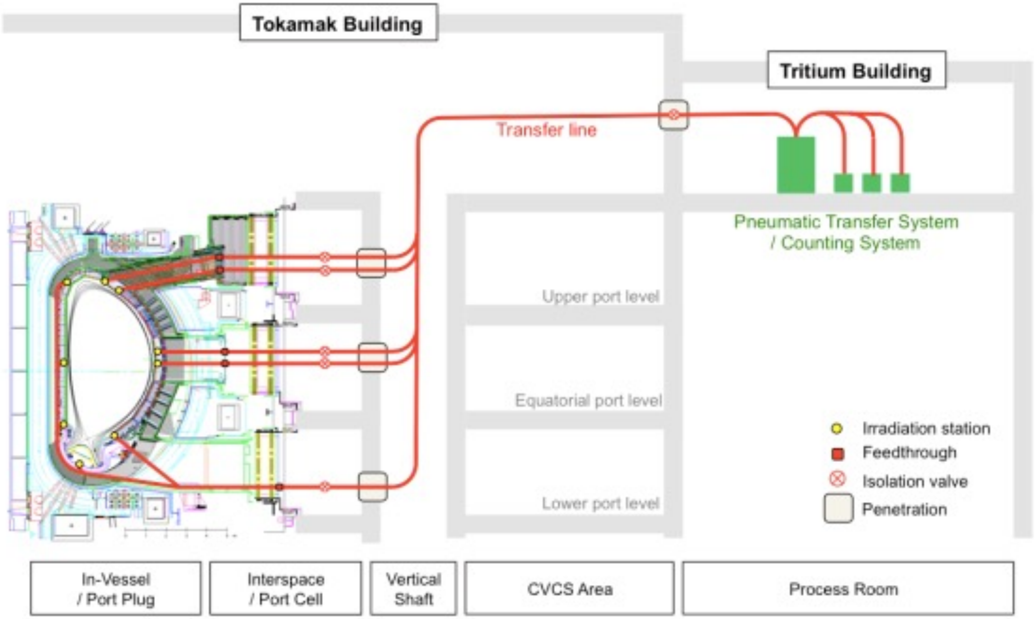

KSTAR NAS

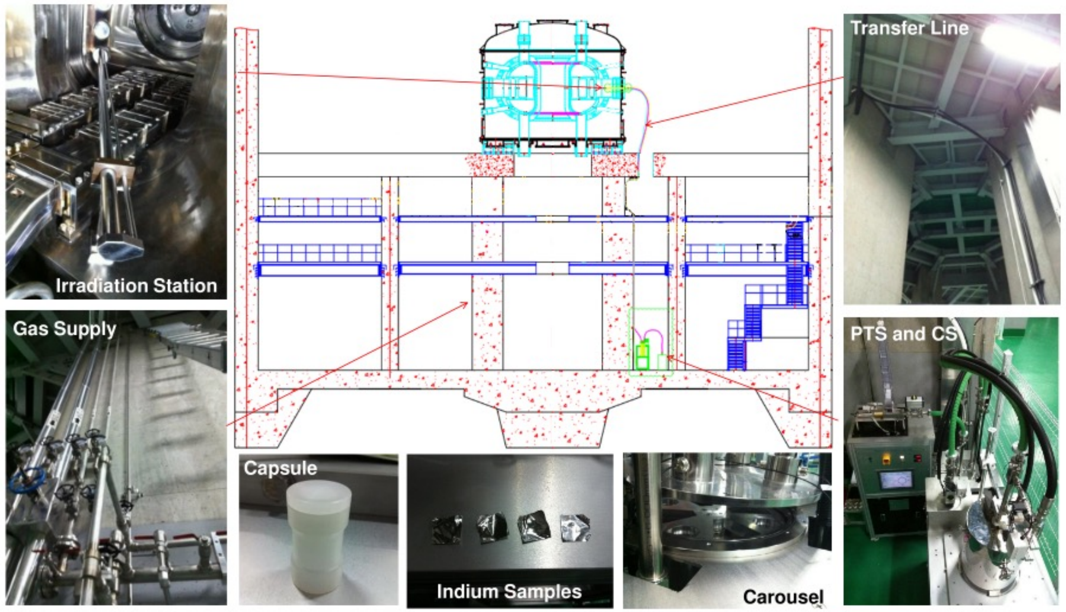

- **ITER prototype NAS diagnostic system has been used at KSTAR.**
- **Fusion-neutron emission rate has been measured quantitatively.**
  - ✓ **2.45 MeV D-D neutron: ~10^{14} n/s**
  - ✓ **14.1 MeV D-T neutron: ~10^{11} n/s**
- **NAS database is being constructed to verify neutron budget of KSTAR plasmas.**

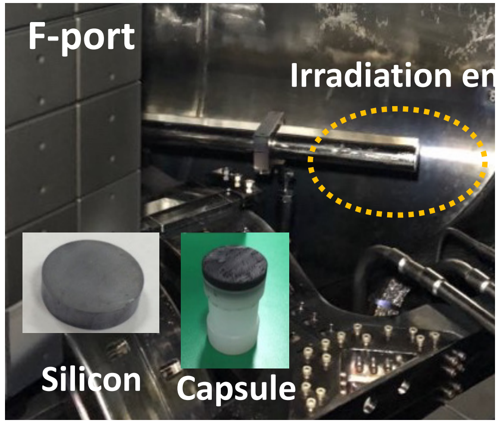

Application of Neutron Diagnostics

Measurement examples (Comparison with TRANSP calculations & Triton burnup study)

➢ **Quantitative neutron rate measurements combined with the NAS diagnostic**

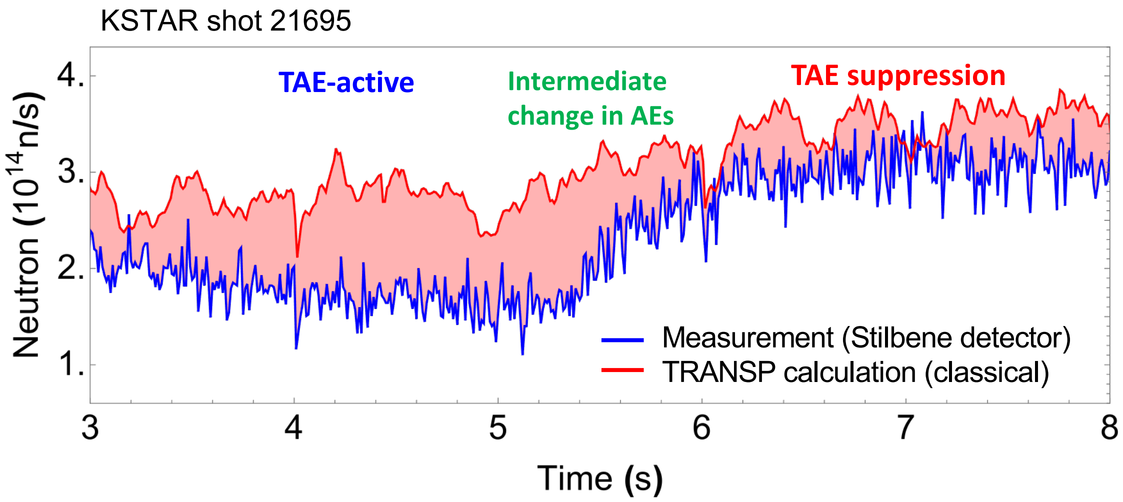

- **Stilbene detector signal → calibrated with the NAS measurements and database → Convert to the quantitative value → Comparison with TRANSP calculations**

➢ **Triton burnup measurement by the Scintillating-Fiber (Sci-Fi) detector**

$$d + t \rightarrow {}^4_2He(3.5\ MeV) + \underline{n(14.1\ MeV)}$$

From d-d fusion (E_{birth} = 1 MeV)

Background plasma

$$TBR = \frac{Y_{n\text{-}dt}}{Y_{n\text{-}dd}}$$ **(ratio between D-D & D-T neutron rates)**

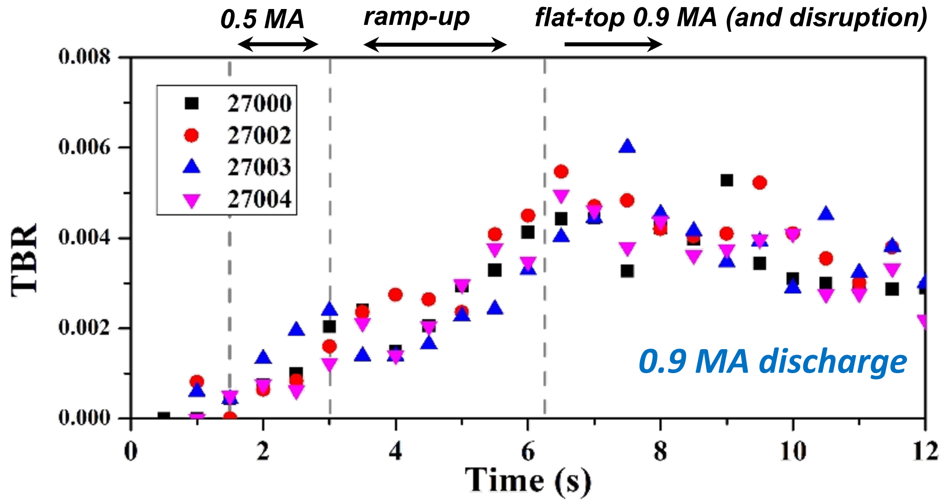

- **Time-dependent triton burn-up ratio (TBR) measurements in high I_P experiments**
- **TBR in KSTAR ~ 0.5%**

Summary

EP experiments on KSTAR

- **Fast-ion loss associated with the 3-D field applications**
  De-phasing RMP is able to reduce the fast-ion loss with approaching to the ELM suppression states.
- **Alfvén eigenmode control test**
  ECCD and 3-D field applications stabilize the TAEs with keeping the performance high.
- **Triton burnup study**
  Fusion-born triton burnup ratio has been measured (~ 0.5%) in KSTAR deuterium higher-performance plasmas.

EP diagnostics on KSTAR

- **Fast-ion loss detector**
  Scintillator-based detector system, the ex-vessel telescopic optics and the wound optical-fiber guide
- **Fast-ion D_α spectroscopy**
  The array of fast-ion charge-exchange doppler spectroscopy measures fast-ion density profiles.
  Eventually, will be used for the fast-ion velocity-space (or phase-space) tomography.
- **Neutron diagnostics**
  Scintillator-based PMT detectors, Sci-Fi detector for measuring D-T neutrons, Neutron activation system (NAS) for the quantitative neutron budget in KSTAR

Thank you!

KSTAR experiment website:
https://kstar.kfe.re.kr

한국핵융합에너지연구원
KOREA INSTITUTE OF FUSION ENERGY